Hochschule für Angewandte
Wissenschaften Hamburg
Hamburg University of Applied Sciences

Hamburg University of Applied Sciences
Faculty Life Sciences
Department Biotechnology

Master thesis

Impact of buffer salts on protein-protein-adsorber interactions by using *E. coli* host proteins in ion exchange frontal chromatography

Jana Otte

Pharmaceutical Biotechnology

27.04.2018

1. Advisor: Prof. Dr. Anspach, Hamburg University of Applied Sciences

2. Advisor: Prof. Dr. Cornelissen, Hamburg University of Applied Sciences

Abstract

This master thesis investigated the impact of buffer salts on protein-protein-adsorber interactions in ion exchange chromatography. Six buffers with different properties were chosen as well as two proteins, lysozyme and BSA, which are different in size and charge. To relate to practice, host cell proteins from *E. coli* were used. For the determination of the binding behaviour, the zonal and frontal chromatographic method were applied. During the zonal chromatography it could be observed that through protein-protein interactions, proteins were adsorbed which carried the same charge as the stationary phase. The received breakthrough curves from frontal chromatography gave information about the dynamic and static binding capacity. Further the dependency of the charge and ionic strength of each buffer on the binding capacities were investigated. To this end, the molarity and the pH was adjusted. Significant differences in the DBC value for each protein solution could be observed. The results showed that the assumptions found in literature [Herrmann, 2002] can´t be applied directly and that more parameters need to be considered individual. In this process several proposals from different sources of literature were applied regarding protein interactions [Rösch et al, 2016], zeta potential [Burns et al., 1999], ionic strength [Salgin et al., 2012] and the influence of the pH [Shi et al, 2005]. It was revealed that the protein size and the formation of protein complexes have a great impact on the breakthrough curve. Through different types and concentrations of buffer salts and changes of the pH, the protein adsorption and therefore the form of the breakthrough curve can be influenced. This impact is reflected rather in the dynamic binding capacity than in the static binding capacity. The results also revealed that it is from advantage to use salt ions which carry the same charge as the desired protein to achieve a higher dynamic binding capacity. Concerning the buffer salt concentration, not only a too high buffer salt concentration (50 mM) led to a decrease of the dynamic binding capacity but also a too low concentration (10 mM). Regarding the pH, the change of the pH from 6.5 to 7.5 enhanced the interaction between BSA and lysozyme (expressed through an increased dynamic binding capacity) because of the more negative net charge of BSA. Especially the protein interactions would make it more difficult to isolate one protein from a protein mixture.

Contents

List of Symbols

Abbreviations

Bis-Tris	bis(2-hydroxyethyl)amino-tris(hydroxymethyl)methane
BSA	Bovine serum albumin
BTC	Breakthrough curve
CM	Carboxymethyl
DEAE	Diethylaminoethyl
E. coli	*Escherichia coli*
FF	Fast flow
HCP	Host cell protein
HAS	Human serum albumin
IEXC	Ion exchange chromatography
kDa	kilodalton
LYS	Lysozyme
M	Maker
MES	2-(*N*-morpholino)ethanesulfonic acid
NaCl	Sodium chloride
NaOH	Sodium hydroxide
P	Peak
pI	Isoelectric point
SDS-PAGE	Sodium dodecyl sulfate polyacrylamide gel electrophoresis
SEC	Size exclusion chromatography

Greek symbols

α	Degree of dissociation	1
v	Kinematic viscosity	St

Indices

0	Input value
break	Breakthrough

Latin symbols

AU	Absorption units	1
AV	Area units	mAU*ml
c	Concentration of solution	mg/ml
CV	Column volume	ml
DBC	Dynamic binging capacity	mg/ml
pH	Negative of the base 10 logarithm of the ‘proton concentration’	1
pK_A	Negative of the base 10 logarithm of the dissociation constant	1
SBC	Static binding capacity	mg/ml
V	Volume	ml

1. Introduction

An important position in pharmaceutical industry is nowadays occupied by drugs which are produced through recombinant methods. With a share of 30 billion US$, protein drugs or biopharmaceuticals are a very promising alternative in treating diseases like cancer and auto-immune diseases [Ratnaparkhi, Chaudhari & Pandya, 2011] compared to conventional drugs based on chemical structures which are not found in the human body. Biopharmaceuticals however can be modified in a way that they structurally mimic human compounds and therefore lower the risk of side effects [Sekhon, 2010]. Hence, the purity of the final product is of great importance, too. This is guaranteed through purifications and downstream methods, such as chromatography [Dismer, Petzold & Hubbuch, 2008]. Chromatography combines many advantages, such as the wide variety of separation methods (e.g. affinity, size exclusion and ion exchange chromatography), high-resolution purification and high purity standards. Characteristics like the size, density, charge and hydrophobic interactions can therefore be utilized. At the same time, it represents the costliest part of the protein production process due to the high purity requirements of the final product which can be up to > 99% [Freitag, 2014]. During purification not only DNA, endotoxins, viruses, host cell proteins and cell debris must be removed, but also products which are misfolded or carry the wrong post-translational modification and thus are similar to the final product. To achieve this, a complex cascade of different methods is necessary. In this connection ion exchange chromatography, in form of anion or cation exchanger, is often used as a polishing step [Hanke & Ottens, 2014]. So far, researches have mainly focused on the characterization and behavior of different adsorber resins, but only a few investigated other influences, such as ionic strength or type of salt ions [Disemer & Hubbuch, 2007]. Therefore, this master thesis will focus on the impact of buffer salts on protein adsorption by using ion exchange frontal chromatography. To simulate more realistic industrial conditions, two different proteins (BSA and lysozyme), as well as a mixture of many proteins (BSA and host cell proteins) were applied on the column at the same time. Regarding the buffers, six salts with different properties such as charge, size and pK_A were chosen. Because of the opposed charge of BSA^+ and $lysozyme^-$, both an anion and a cation exchanger were used. For the evaluation of the impact of buffer salts on the protein-protein-adsorber interactions, the dynamic and static binding capacity (DBC and

SBC) was chosen. The DBC and SBC can be determined by means of frontal chromatography. To get an understanding of the interaction of the proteins among themselves, zonal chromatography was used as an additional method. During the experiments either the molarity or the pH of the buffer salt was changed. As values for the molarity 10 mM, 20 mM, 30 mM and 50 mM were chosen and for the pH 6.5 and 7.5.

2. Theoretical background

Chromatography (Greek *chroma*: 'color' and *graphein*: 'to write') is a method for the separation of sample components using a stationary and a mobile phase which was first invented and developed at the beginning of the 20th century by Mikhail Tswett. Tswett used this technique initially for the separation of colored plant pigments. Since then, it took almost 30 years until its potential was rediscovered by German scientists as liquid chromatography (LC). Before the method of 'washing out' the bound component was introduced in the mid-1930s, the packed column material had to be removed after every sample application and the pure components had to be removed by extraction [Robards, Haddad & Jackson, 2004]. By 1943, a Swedish scientist developed three modes of chromatography: frontal, elution and displacement. During the following years, further chromatographic methods have been developed, as for example ion exchange chromatography (IEXC), gas chromatography (GC), size exclusion chromatography (SEC) and the high-performance liquid chromatography (HPLC) [Lundanes Reubsaet & Greibrokk, 2014]. In today's industry, chromatography plays an important part in the purification and downstream process of proteins produced by recombinant DNA technology [Carta & Jungbauer, 2010]. A method which will be further discussed in the following chapter is the ion exchange chromatography.

2.1 Ion exchange chromatography

Ion exchange chromatography is a method based on the interaction of a charged analyte (amino acids, peptides and proteins) with an oppositely charged carrier (matrix or stationary phase) (see Figure 2.1). Two different ion exchangers are known: anion and cation exchanger. They can be characterized by their properties of acidic or basic functions and by their ability to attract ions. Anion exchangers have a positively charged surface and therefore attract negatively charged ions. With the cation exchanger, the opposite is realized. One possible way of controlling the separation is changing the ionic strength of the solutions and therefore influencing the interaction between the stationary phase and the analyte. For the

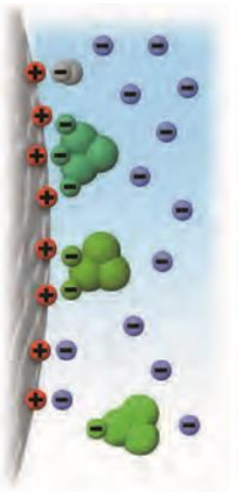

Figure 2.1: Separation principal of an IEXC [GE Healthcare].

elution of the analyte from the stationary phase either the salt concentration or the pH value can be changed. Whether one uses an anion or cation exchanger is depending on the pH stability of the analyte and its isoelectric point (pI: pH at which the net charge is zero). When choosing a pH above the pI, the analyte will be negatively charged. At a pH below the pI the analyte will be positively charged. Besides the charge of the analyte and the pH used, the composition of the matrix is of importance, too. The matrix can be based on synthetic resins, inorganic compounds or polysaccharides (e.g. Sepharose) and can be nonporous or porous. The characteristics of the matrix can have a great influence on the capacity, efficiency, recovery and stability of the process. Depending on the functional groups bound to the matrix, ion exchangers can be classified as weak and strong. This only refers to the pK_A value of those functional groups and doesn't characterize the strength of the binding. Most commonly used are carboxymethyl- (CM) and diethylaminoethyl- (DEAE) groups [Inamuddin & Luqman, 2012].

2.1.1 Frontal chromatography

Due to the simplicity and accuracy, frontal chromatography is an often-used chromatographic mode [Casez, 2001] in which a continuous flow of sample is used to determine the binding capacity of a column depending on analyte and buffer. To this end the sample volume can be many times greater than the column volume. As the sample is continuously applied onto the column, it interacts with the available binding sites of the matrix. Those binding sites slowly become saturated until no sample can be bound anymore. This leads to the typical breakthrough curve (BTC) (see Figure 2.2) [Grushka & Grinberg, 2014]. The course of the breakthrough curve is plotted against the time or volume and the normalized inlet concentration of the sample (c/c_0). At the beginning the sample is completely adsorbed ($c/c_0 = 0$) and with increasing absorbance corresponding to an increasing protein concentration *c* at the column outlet, the course of the curve comes closer to the inlet concentration ($c/c_0 = 1$). This method can be used for the determination of the static and dynamic binding capacity [Sepahi et al., 2014]. Following factors can have an influence the breakthrough curve: functional groups of the sample, diffusion and mass-transfer kinetics and the capacity of the column itself [Casez, 2001].

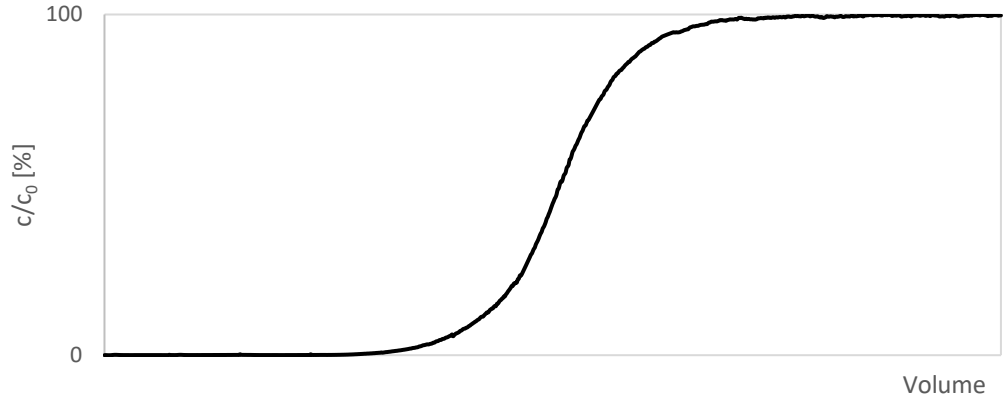

Figure 2.2: Example of frontal chromatography with a breakthrough curve.

2.1.2 Zonal chromatography

Zonal chromatography, or zonal elution, is a method which is normally used in affinity chromatography or HPLC for studies of the binding behavior of e.g. proteins. Thereby a defined amount of known sample is injected onto a column in the presence of a buffer [Grushka & Grinberg, 2014]. For the elution of the sample, a linear gradient from 0% to 100 % of the same buffer with an additional and higher salt concentration is used (see Figure 2.3). Commonly a washout phase at the beginning and delay at the end of the gradient is added. The salt ions (e.g. Na^+ or Cl^-) compete with the ligand of the column and thus displace the analyte over the course of the gradient leading to the typical peak [Inamuddin & Luqman, 2012].

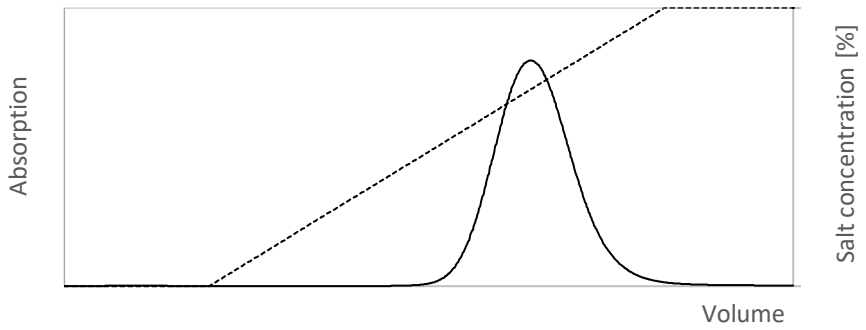

Figure 2.3: Example of a zonal elution peak with linear salt gradient and a gradient delay.

2.2. Binding capacity

2.2.1 Dynamic binding capacity

For the optimization of a chromatographic process it can be necessary to determine the dynamic binding capacity (DBC). A specified percentage of the breakthrough curve can be chosen (c/c_0 = 0.01, 0.05 or 0.1) [Carta & Jungbauer, 2010]. This point marks the volume which is used to calculate the DBC (see Figure 2.4). The multiplication of the volume with the sample concentration results in the mass of the sample which has been applied onto the column until this specific breakthrough. Expressed in an equation:

$$DBC = \frac{c_0 \times V_{break}}{V_{column}} \quad (2.1)$$

where DBC is the dynamic binding capacity (mg/ml), c_0 is the concentration of the sample in solution (mg/ml), and V_{break} the volume of the point of breakthrough (ml) and V_{column} the volume of the column (ml). In the end the DBC of a protein can be dependent on many factors such as the flow rate, the type of stationary phase, protein size and charge, the ionic strength of the buffer and the pH. A good DBC leads to a decreases of process time, protein loss and costs [Sepahi et al., 2014].

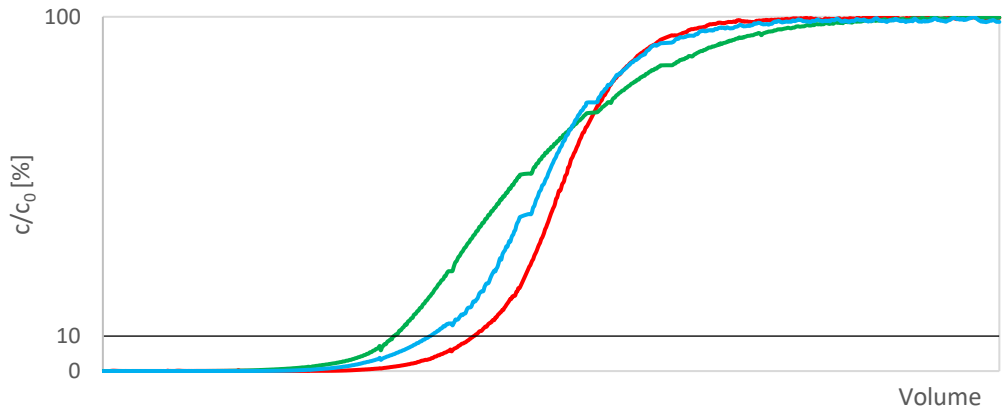

Figure 2.4: Specific percentage (10 %) of the breakthrough curve leading to a different DBC of the green, blue and red curve.

2.2.2 Static binding capacity

The static binding capacity (SBC), also referred to as equilibrium binding capacity, is the maximum amount of protein which can be bound at a given protein concentration until every binding site is occupied. In case of a symmetrical breakthrough curve, it can be calculated by the point of the breakthrough curve at which the binding capacity is at

equilibrium. At this point it is simply multiplied with the protein concentration c_0. In case of an asymmetrical curve a numeric calculation is necessary [Anspach, 2012].

$$\int_a^b f(x)dx \approx \frac{f(a)+f(b)}{2}(b-a) \quad (2.2)$$

Equation (2.2) can be used for a relatively exact approximation of the area under the curve which is needed to be subtracted from the rectangle calculated from the height of the plateau multiplied with the retention volume, resulting in the area above the curve (see Figure 2.5). This value equals the static binding capacity. For the calculation a complete breakthrough curve is necessary.

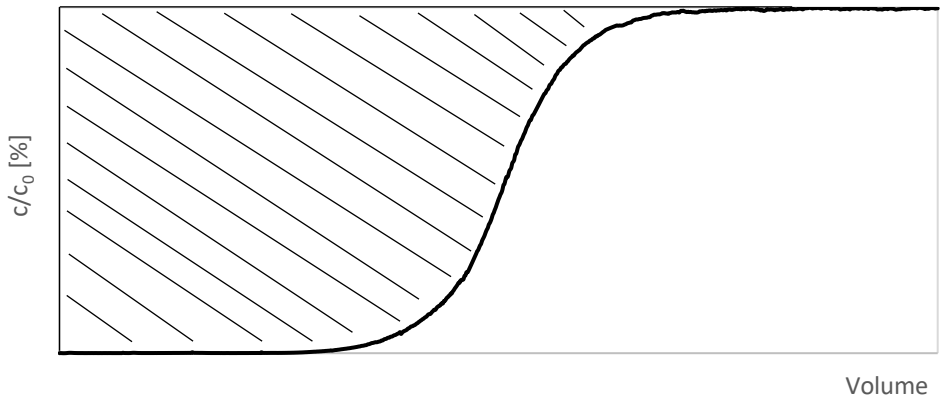

Figure 2.5: Example of a breakthrough curve for the determination of the SBC. The shaded area above the curve equals the SBC.

2.3 Zeta potential

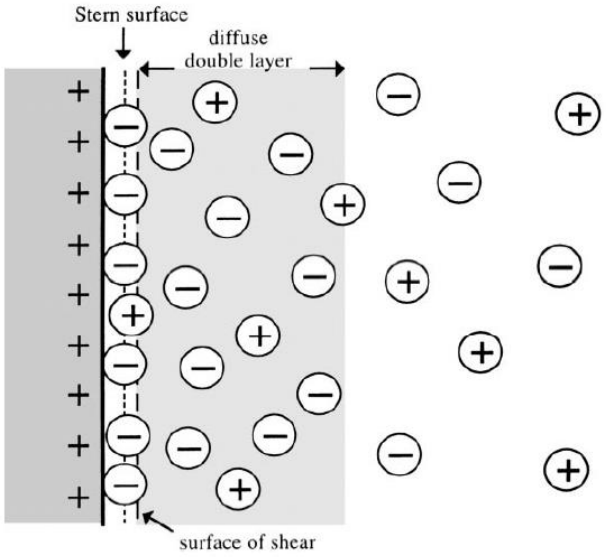

Figure 2.6: Schematic representation of ion distribution near a positively-charged surface [Burns and Zydney, 1999].

Since ion exchange chromatography is based on electrostatic forces between a biomolecule and an adsorber, the zeta potential can be used to describe their interactions. More precisely, the zeta potential reflects electrostatic interactions between a surface charge and a liquid containing functional groups. Those functional groups can dissociate onto the surface or the surface adsorbs ions from the solution. The zeta potential itself forms at the interface of the liquid and the solid surface. The zeta potential can be influenced in different ways by changing the pH of the aqueous phase or the dissociation of functional groups. The mechanisms of ion adsorption itself can also be changed. Moreover, the concentration and type of salts in the liquid phase have an effect on the electrical charge and therefore on the zeta potential [Salgin, Salgin & Bahadir, 2012]. Figure 2.6 displays a schematic distribution of ions near a positively charged surface. This liquid layer with an increased concentration of counterions is called the Stern layer. Those ions are adsorbed to the surface. The ions in the outer region form the diffuse double layer. They are less firmly adsorbed to the surface. A third region is the surface of shear, located just beyond the Stern surface. Its electric potential is defined as the zeta potential and is generally used to characterize the electric properties of surfaces [Burns & Zydney, 1999] and the electrostatic interaction between two charged surfaces [Salgin et al., 2012].

2.4 Buffers

Buffer solutions have the purpose of keeping the pH stable over a lengthy period of time even after the addition of acids or bases. Buffer solutions consist out of weak acid (HA) and its conjugated base (A^-). If the ratio of weak acid and conjugated base is 1:1, it can also be expressed through $pH=pK_A$ [Mortimer & Müller, 2010]. When choosing a buffer, it is of importance to know at which pH the process should run because the pH itself has already a great influence on the separation of peptides and proteins. Further the pK_A value of the buffer should be close to the working pH. But the pH should differ at least one value from the pI of the analyte [Inamuddin et al., 2012]. Besides the pH the ionic strength and electrostatic interactions of a buffer have also an influence on the protein adsorption. The ionic strength may lead to a competitive binding or shielding effect. So, by increasing the salt concentration and thereby the number of ions, those ions may bind onto the charged functional groups of the stationary phase and thus replace the adsorbed protein. There is also the risk, that the salt ions shield the charge groups of the protein surface and thus prevent the interaction between the protein and the stationary phase of the column. Further di- and tri-valet ions can have a negative influence on the zeta potential of the ion exchanger or can affect the surface charge of the protein [Niu, 2015].

For the further evaluation of the buffers, the degree of dissociation has been examined. Therefore, the Henderson-Hasselbalch equation (2.3) was applied. Usually this equation is used for the calculation of a pH, but by rearranging the equation the dissociation quotient $c(HA)/c(A^-)$ can be calculated (2.4). With the equation (2.5) the degree of dissociation (α) of the buffer and thus the distribution of ions can be determined [Mortimer & Müller, 2010].

$$pH = pK_A - lg\frac{c(HA)}{c(A^-)} \quad (2.3)$$

$$\frac{c(HA)}{c(A^-)} = 10^{(pH - pK_A)} \quad (2.4)$$

$$\alpha = \frac{c(A^-)}{c(HA) + c(A^-)} \quad (2.5)$$

During the experiments six different buffers will be used and examined. The selected buffers all have different properties regarding their charge, molecular mass and pK_A value(s).

Bis-Tris

The IUPAC name of Bis-Tris is bis(2-hydroxyethyl)amino-tris(hydroxymethyl)methane. It has a molecular mass of 209.24 g/mol, a pK_A of 6.46 and can be used in a buffer range from 5.8 to 7.2 [AppliChem.com]. At a pH of 6.5 almost the half of the Bis-Tris molecules in the buffer solution are protonated (9.54 mM of 20 mM).

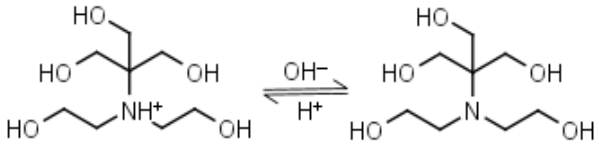

Figure 2.7: Dissociation step of Bis-Tris [reachdevices.com].

Imidazole

Imidazole is an aromatic heterocycle with three C- and two N-atoms and is often used as a buffer during enzymatic reactions or for the denaturation of DNA. It has a pK_A of 6.95 can be used in a buffer range from pH 6.2 to 7.8. Compared to the other used buffers, Imidazole is relatively small with a molecular mass of only 68.08 g/mol [AppliChem.com]. Imidazol is mostly protonated at a pH of 6.5 (14.76 mM of 20 mM) and weak protonated at pH 7.5 (4.40 mM of 20 mM).

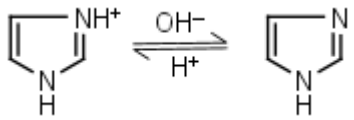

Figure 2.8: Dissociation step of imidazole [reachdevices.com].

MES

MES is the abbreviation of 2-(*N*-morpholino)ethanesulfonic acid. It is a zwitterion with a positively charged amino group and a negatively charged sulfonyl group. MES has a molecular mass of 195.20 g/mol. It can be used at a buffer range from 5.5 to 6.5 and with its pK_A value of 6.10 [AppliChem.com]. The buffer molecules are mainly present as monovalent anions at pH 6.5 (14.31 mM of 20 mM). This share increases at pH 7.5.

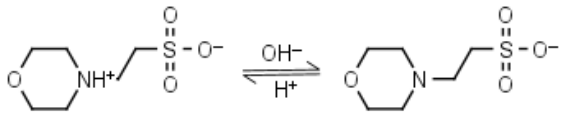

Figure 2.9: Dissociation step of MES [reachdevices.com].

Sodium acetate trihydrate

Sodium acetate is the sodium salt of acetic acid and is used in the food industry as a preservative (E262) for fruits and vegetables [enius.de]. It has one pK_A value at 4.76 and can be used at a relatively low pH range of 3.7 to 5.6. The molecular mass is 136.08 g/mol. [AppliChem.com].

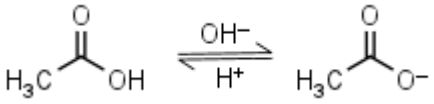

Figure 2.10: Dissociation step of acetic acid [reachdevices.com].

Calculation by using equation (3) results in a dissociation quotient of 54.95 and thus leading to a distribution of 0.36 mM neutral charged and 19.64 mM simply negative charged molecules at a concentration of 20 mM and pH of 6.5

Sodium carbonate

Sodium carbonate is the disodium salt of carbonic acid with a molecular mass of 105.99 g/mol and is widely used in the industry. It has two pK_A values at 6.35 and 10.33 and is usable at a buffer range of 6.0 to 8.0 [AppliChem.com]. At a pH of 6.5 the dissociation quotient is 1.413. This means that 11.71 mM of 20 mM are present as monovalent anions. At pH 7.5 the number of monovalent anions increases further (18.68 mM).

$pK_{A,1}$: 6.35 $\quad H_2CO_3 \Leftrightarrow HCO_3^- + H^+$

$pK_{A,2}$: 10.33 $\quad HCO_3^- \Leftrightarrow CO_3^{2-} + H^+$

Sodium dihydrogen phosphate dihydrate

Because of its broad buffer range from 5.8 to 8.0 sodium phosphate is an often-used buffer system in biochemistry and has a molecular mass of 156.01 g/mol [Herrmann, 2002]. Due to its three pK_A values, the following chemical equations result from this:

$pK_{A,1}$: 2.15 $H_3PO_4 \Leftrightarrow H_2PO_4^- + H^+$

$pK_{A,2}$: 7.20 $H_2PO_4^- \Leftrightarrow HPO_4^{2-} + H^+$

$pK_{A,3}$: 12.33 $HPO_4^{2-} \Leftrightarrow PO_4^{3-} + H^+$

At the pH of 6.5 the sodium phosphate molecules are mainly present as monovalent anions (16.67 mM) and 3.33 mM as divalent anions in a 20 mM solution.

2.5 Proteins

2.5.1 Bovine serum albumin

Bovine serum albumin (BSA) is a protein which is derived from cattle and shares a 76% sequence identity with human serum albumin [Huang, Kim & Dass, 2004]. BSA is present in blood plasma where it works as a depot and transport protein for amino and fatty acids, salts, hormones and also for drugs and pharmaceuticals. The molecular mass of BSA is about 66.200 Da with a single polypeptide chain consisting of 583 amino acids [Patra, Santhosh, Pabbathi & Samanta, 2012]. The tertiary structure is arranged in a heart-shaped form and is composed of three helical domains which are similar to each other (I, II and III) Further each domain consist of two subdomains (A and B) which are all connected to each other with 17 disulfide bonds (see Figure 2.11) [Majore et al., 2012]. The calculated isoelectric point of BSA is 5.4 and the measured pI is 4.8, thus BSA is negatively charge at a pH of 6.5. The calculated net charge of BSA at this pH is -13. [Shi, Zhou & Sun, 2005].

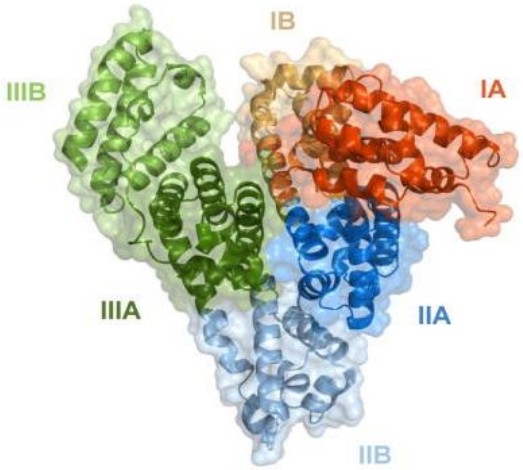

Figure 2.11: Domain structure of BSA [Majorek et al., 2012].

2.5.2 Lysozyme

Lysozyme from hen egg-white has a molecular weight of approximately 14.3 kDa and consist of a singled polypeptide chain of 129 amino acid residues with four crossed linked disulfide bridges (see Figure 2.12) [Phillips, 1967]. Lysozyme is often used for the hydrolysis of cell wall, especially of gram-positive microorganisms like *E. coli*. The enzyme used from SIGMA-ALDRICH shows activity in a pH range of 6.0 to 9.0 and has a pI of 11.35, thus it is positively charged at a pH below the pI [sigma-aldrich.com]. Lysozyme has several charged groups which are located on the surface of the molecule. The largest share is made up by arginine, lysine and aspartic acid. Lysine and arginine carry a positive charge when using a pH below 7 during ion exchange chromatography [Niu, 2015].

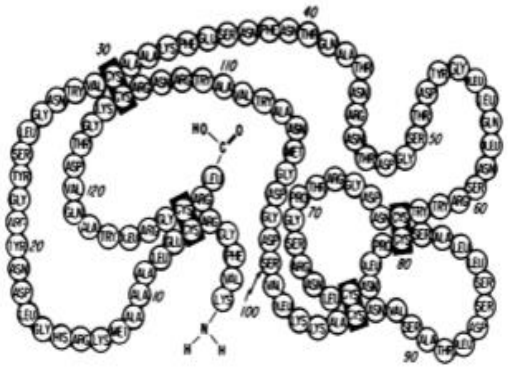

Figure 2.12: Lysozyme [Phillips, 1967].

2.5.3 Host cell proteins

Each organism has a different set of host cell proteins (HCPs). The function of HCPs which are encoded and produced by the host reaches from growth to survival and cellular processing. Some HCPs are just carried along as “baggage” and are non-essential. HCPs can be modified with post-translational modifications just as recombinant products. During the production of biopharmaceuticals, in form of recombinant proteins, the presence of HCPs is undesirable. Thus, great effort is made in removing them during purification [Wang, Hunter & Mozier, 2009]. Because HCPs are a mixture of different proteins, there is no unitary pI. This means that during ion exchange chromatography at a pH of 6.5 only a certain share of proteins will bind to the column.

2.6 Stationary phase

2.6.1 CM Sepharose Fast Flow

The cationic ion exchanger consists of Sepharose® (tradename for Separation-Pharmacia-Agarose) which is extracted from seaweed. As seen in Figure 2.13, agarose is a linear polymer consisting of alternation D-galactose which is liked to a 3,6-anhydro-L-galactose. The matrix is composed of 6% highly crosslinked agarose [Herrmann, 2002].

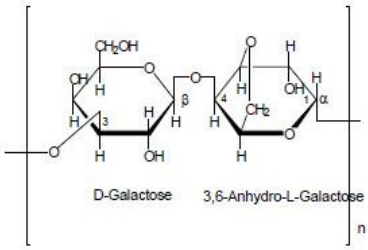

Figure 2.13: Agarose consisting of alternating D-galactose and is liked to a 3,6-anhydro-L-galactose [sigmaaldrich.com].

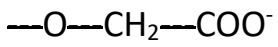

Figure 2.14: Chemical structure of the functional group carboxymethyl (CM) [gelifesciences.com].

In combination with the ligand carboxymethyl (CM) (see Figure 2.14), the type of ion exchanger can be described as weak cation exchanger. The bead size varies from 45 to 165 µm with an average particle size of 90 µm. The total ionic capacity is 0.09 to 0.13 mmol H^+/ml and a pH stability is given from 4 to 13. The DBC of the coulmn is 50 mg ribonuclease A/ml medium. CM Sepharose FF can be used for method scouting, group separation or sample concentration [gelifesciences.com].

2.6.2 DEAE Sepharose Fast Flow

The weak anion exchanger consists also of Sepharose® combined with diethylaminoethyl (DEAE) groups (see Figure 2.15). The bead size diversifies from 45 to 165 µm with an average particle size of 90 µm. Its total ionic capacity is 0.11–0.16 mmol Cl^-/ml and the DBC is 110 mg HSA/ml medium. During working mode, the column has a pH stability from 2 to 12. This type of ion exchanger is used for method scouting, sample concentration and sample clean-up of charged biomolecules [gelifesciences.com].

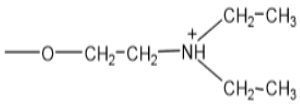

Figure 2.15: Chemical structure of the functional group diethylaminoethyl (DEAE) [gelifesciences.com].

3. Material and Methods

3.1 Equipment and Chemicals

3.1.1 Equipment

Chromatography	ÄKTA Purifier	GE Healthcare
Chromatography	ÄKTA Start	GE Healthcare
Balance	AX623	Sartorius
Balance	BP 2215	Sartorius
Centrifuge	Multifuge 3 S-R	Heraeus
Conductivity meter	HI 8733	HANNA
Dialysis membrane	Spectra/Pro®	SPECTRUM®
ELISA Reader	Multiscan Ascent	Thermo
Magnetic stirrer	MONO DIRECT 30108	VARIOMAG
pH meter	766 Calimatic	Knick
Pump	P-500	Pharmacia
Quartz cuvette	104-QS	Hellma
SDS-PAGE	Mini PROTEAN®	Bio Rad
Spectrophotometer	Ultraspec 2100 pro	Amersham Biosciences
Ultrasound	Sonifier 250	Branson
Vacuum pump	LABOPORT	KNF
Viscometer	50904	SCHOTT Instruments

3.1.2 Chemicals

Aryl/Bisarylamide	Roth
APS	Merck
Bis-Tris	Roth
Ethanol	Roth
Imidazole	Merck
Maleic acid	J. T. Backer
MES	Roth
Sodium acetate trihydrate	Roth
Sodium carbonate	Roth
Sodium chloride	Roth
Sodium dihydrogen phosphate dihydrate	Roth
Roti Blue (5x) /Roti®-Quant Universal	Roth
Roti®-Mark STANDARD	Roth
SDS	Roth
TEMED	Roth
Tris	Roth

3.1.3 Proteins and Stationary phase

HiTrap™ CM FF 1ml	GE Healthcare
HiTrap™ DEAE FF 1ml	GE Healthcare
HiTrap™ Desalting 5ml	GE Healthcare
Albumin, IgG free	Roth, 3737.2
Host cell proteins	*E. coli* MR4616
Lysozyme from chicken egg white	Sigma-Aldrich, 62971-G50-F

3.3 Buffer preparation

Adsorption buffer (Buffer A)

The adsorption buffer is used for the equilibration of the stationary phase and for the protein adsorption itself. The salts were dissolved in distilled water. All buffers have a volume of 500 ml. The adjustment of the pH was performed with hydrochloric acid and caustic soda at a temperature of 21°C. Before usage the buffers were filtered and degassed using a cellulose acetate filter from Sartorius stedim biotech with a pore size of 0.45 µm.

Buffer A	**Concentration**	**Amount**
Bis-Tris	20 mM	1.091 g Bis-Tris 500 ml dest. H_20
Imidazole	10 mM	0.340 g Imidazole 500 ml dest. H_20
	20 mM	0.681 g Imidazole 500 ml dest. H_20
	30 mM	1.021 g Imidazole 500 ml dest. H_20
	50 mM	1.702 g Imidazole 500 ml dest. H_20
MES	10 mM	0.976 g MES 500 ml dest. H_20
	20 mM	1.952 g MES 500 ml dest. H_20
	30 mM	2.928 g MES 500 ml dest. H_20
	50 mM	4.880 g MES 500 ml dest. H_20

Sodium acetate trihydrate	20 mM	1.361 g Sodium acetate trihydrate 500 ml dest. H_20
Sodium carbonate	10 mM	0.530 g Sodium carbonate 500 ml dest. H_20
	20 mM	1.060 g Sodium carbonate 500 ml dest. H_20
	20 mM	1.590 g Sodium carbonate 500 ml dest. H_20
	50 mM	2.650 g Sodium carbonate 500 ml dest. H_20
Sodium dihydrogen phosphate dihydrate	20 mM	1.560 g Sodium dihydrogen phosphate dihydrate 500 ml dest. H_20

Desorption buffer (Buffer B)

The desorption buffer has the same concentration of buffer salts as the adsorption buffer. Additionally, NaCl with a concentration of 1 M was added. Buffer B is used for the elution of bound protein. The volume is 100 ml. The pH was adjusted with hydrochloric acid and caustic soda at a temperature of 21°C. Before usage the buffers were filtered and degassed using a cellulose acetate filter from Sartorius stedim biotech with a pore size of 0.45 µm.

Buffer A + NaCl	**Amount**
Bis-Tris 1 M NaCl	100 ml Bis-Tris 5.844 g NaCl
Imidazole 1 M NaCl	100 ml Imidazole 5.844 g NaCl
MES 1 M NaCl	100 ml MES 5.844 g NaCl
Sodium acetate trihydrate 1 M NaCl	100 ml Sodium acetate trihydrate 5.844 g NaCl
Sodium carbonate 1 M NaCl	100 ml Sodium carbonate 5.844 g NaCl
Sodium dihydrogen phosphate dihydrate 1 M NaCl	100 ml Sodium dihydrogen phosphate dihydrate 5.844 g NaCl

3.4 Sample preparation

3.4.1 BSA and Lysozyme

For the protein solution with BSA and lysozyme, the desired weight was weighted and afterwards dissolved in the adsorption buffer. Two different protein concentrations were used. For BSA the concentration was 1 mg/ml whilst an anion or cation exchanger was applied. The concentration of lysozyme was 1 mg/ml with the anion exchanger and 2 mg/ml when using the cation exchanger to receive a complete breakthrough curve. A volume of 170 ml was prepared for each run.

3.4.2 Host cell proteins

The *E. coli* cells (MR4616) were received from Janet Hirsch (HAW Hamburg, lab for bioprocess automation).

Table 3.1: 1L of PBS solution contains following chemicals

Mass	Chemicals
8.0 g	Sodium chloride (NaCl)
0.2 g	Potassium chloride (KCl)
1.78 g	Sodium dihydrogen phosphate dihydrate ($Na_2HPO_4 \bullet 2\ H_2O$)
0.27 g	Potassium dihydrogen phosphate (KH_2PO_4)

Cell disruption

For the cell disruption of E. coli, the ultrasound method was chosen. Therefor the device Sonifier 250 and a coin shaped sonotrode were used. The cell suspension 15% (w/v) wet cells in PBS (see Table 3.1) was filled into a rosette cell, which is placed in ice water, and then treated with ultrasound for 8 minutes at a constant sonication. After the disruption the suspension was centrifuged (Multifuge 3 S-R) for 20 min at 5000 rpm for the removal of cell debris. For the storage, centrifuge tubes were filled with 5 ml of the stock solution and then placed in a freezer at -20°C.

Dialysis

Dialysis was used for the change of the buffer system in which the HCP (V < 1 ml) should be dissolved. Therefore, the protein solution was filled into a dialysis membrane tube which was soaked in distilled water at room temperature for 30 min before usage. Then at both ends of the dialysis tube clamps were placed, leaving 10-20% extra tubing length for air head space insuring buoyancy above the rotating stir bar. The dialysis membrane was positioned into a beaker in which the buffer volume should be ≥ 100 times the sample volume. The dialysis buffer was changed 3 times, continuing overnight. After the last change, the dialysis should last another two hours before removing the sample from the tube.

SEC

For changing the buffer solution of small sample volumes (V ≈ 1 ml) an alternative method is the size exclusion chromatography. Therefor the HiTrap™ Desalting 5ml column and the ÄKTA start was used. For this method the equilibration and elution buffer are identical.

Step	Volume	Description
Equilibration	1 CV	Equilibration of the column with buffer
Sample injection	1 ml	1 ml protein sample is applied on the column
Elution	2 CV	Elution with the same buffer as equilibration

3.5 Experimental equipment

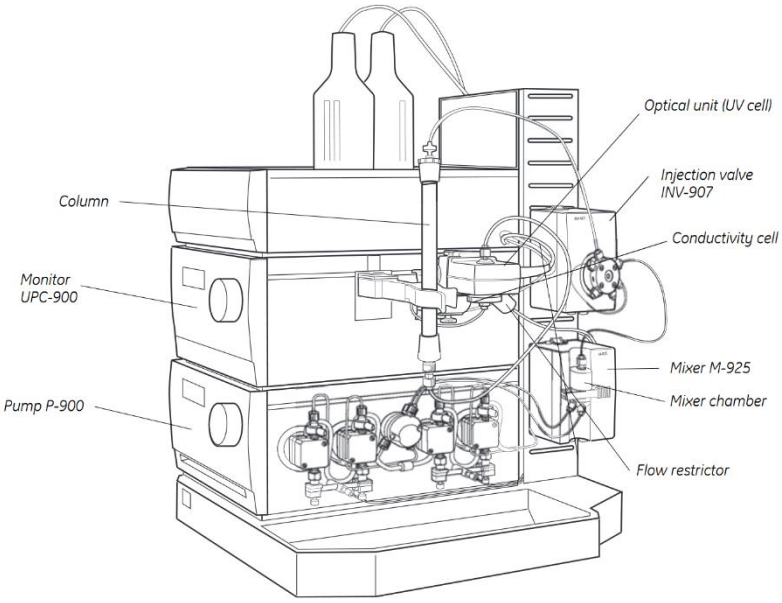

Figure 3.1: Schematic set up of the ÄKTApurifier [gelifesciences.com].

Figure 3.1 shows the plan of an ÄKTApurifier with a pump unit (P-900) and a monitor (UPC-900). The ÄKTApurifier is connected to the external pump P-500 from Pharmacia via an auxiliary (AUX) connection. The facility is linked to a computer and can be controlled by the program UNICORN. The P-500 can only be set to 0 (stop) and 1 (run) by the program. Therefore, the flow rate is adjusted directly at the pump as 60 ml/h.

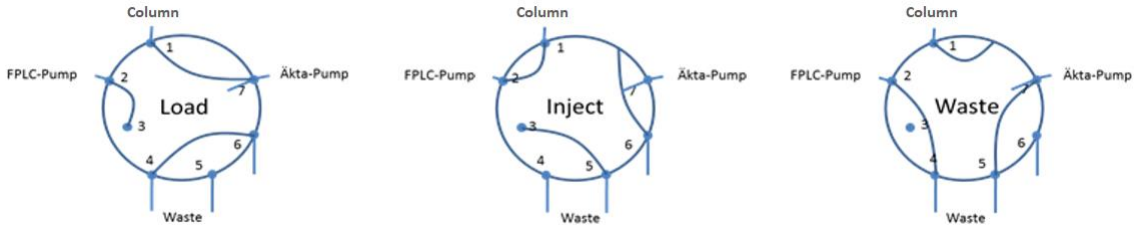

Figure 3.2: Valve (INV 907) positions of the ÄKTApurifier for different experimental methods.

For the application of large sample volumes, which is the case during frontal chromatography, the following positions and connections of the valves are possible (see Figure 3.2). During Load position the flow over the column is regulated by the ÄKTA pump e.g. for equilibration or a salt gradient. By switching to the Inject position, it is possible to apply the sample volume by an external pump. At Waste position, all liquids are pumped into a waste vessel without connection to the column.

3.6 Experimental methods

For the analysis of the protein behavior different methods were chosen which are described in the following section. Each method worked with a flow rate of 1 ml/min. At the beginning of every method queue the P-500 was prewashed with the protein solution and the pumps A1 and B1 of the ÄKTApurifier were washed with the adsorption and desorption buffer. The "Leergradient" served as a minor cleaning step for the column. The method queue was structured as follows: Leergradient, zonal, frontal, Leergradient.

Zonal chromatography

Step	Duration	Description
Equilibration	10 min	Equilibration of the column with a new buffer
Sample injection	1 min	1 ml sample protein is applied on the column
Washing	2 min	Washing of the column with equilibration buffer to wash out unbound proteins
Elution	13 min	Change to desorption buffer. Linear increasing salt gradient until 100% with a 3 min delay leading to an elution of the sample protein

Frontal chromatography

Step	Duration	Description
Equilibration	10 min	Equilibration of the column with a new buffer
Sample injection	120 min	Continuous protein application onto the column
Elution	5 min	Change to 100 % desorption buffer leading to an elution of the protein

Leergradient

Step	Duration	Description
Equilibration	10 min	Equilibration of the column with equilibration buffer
Gradient	10 min	Linear increasing salt gradient until 100% desorption buffer is reached
Delay	3 min	Additional washing step with 100 % desorption buffer

Washing of the column

For this procedure, the column was reversed and then washed with 1 M NaOH for 10 minutes at a flow rate of 0.5 ml/min (GE Healthcare recommends washing with at least 4 CV). Every four weeks a centerpoint run was performed to ensure the unchanging quality of the column. Experiments have shown that a column regeneration should be done after eight frontal chromatographic runs. Figure 3.3 shows the centerpoint runs of the CM FF column with LYS (2 mg/ml) and 20 mM phosphate buffer at pH 6.5. The 6th run was performed on the last day. It can be seen that the breakthrough curves remain similar during the entire series of experiments. The same is true for the DEAE column (see Figure 3.4). BSA (1 mg/ml) and 20 mM phosphate buffer at pH 6.5 where set as the standard. A 6th centerpoint couldn´t be realized due to the breakdown of DEAE column during the last test series.

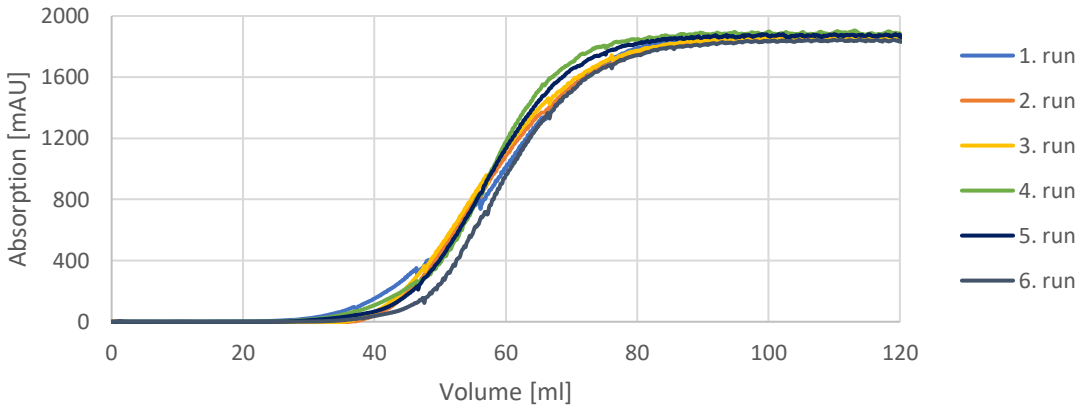

Figure 3.3: Centerpoint runs for the verification of the constant binding behavior of the CM column. Flow rate = 1 ml/min. Buffer A = 20 mM phosphate. pH = 6.5.

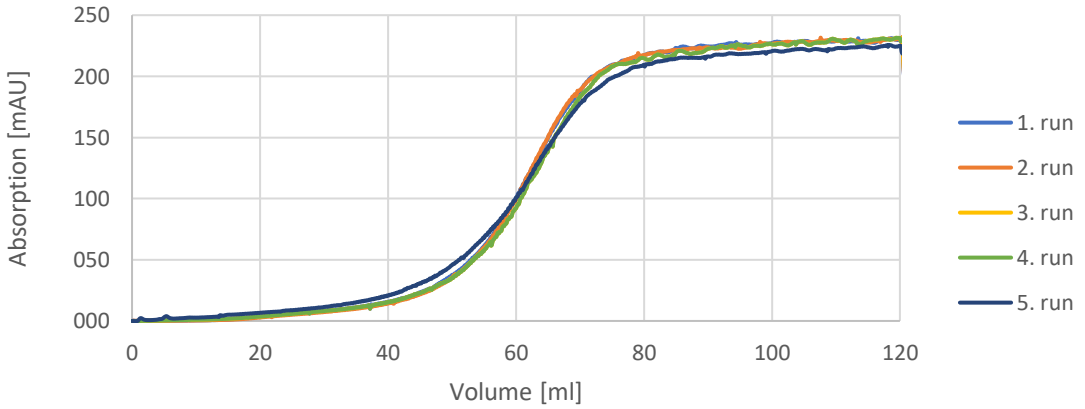

Figure 3.4: Centerpoint runs for the verification of constant binding behavior of the DEAE column. Flow rate = 1 ml/min. Buffer A = 20 mM phosphate. pH = 6.5.

3.7 Analytics

3.7.1 Conductivity

The conductivity was measured by using a conductivity meter of the type HI 8733 (HANNA). For the absorption buffers the following conductivities at a concentration of 10/20/30/50 mM and pH 6.5/7.5 were determined:

Table 3.2: Conductivity of the buffers at 20 mM, pH 6.5 and 7.5

Buffer	Conductivity [mS/cm]	
	pH 6.5	pH 7.5
Acetate	1.80	-
Bis-Tris	0.54	-
Carbonate	3.35	4.16
Imidazole	1.34	0.24
MES	1.02	1.53
Phosphate	2.16	-

Table 3.3: Conductivity of carbonate, imidazole and MES at 10 mM, 30 mM and 50 mM, pH 6.5

Buffer	Conductivity [mS/cm]		
	10 mM	30 mM	50 mM
Carbonate	2.21	5.46	8.82
Imidazole	0.91	1.82	2.98
MES	0.85	1.75	2.41

3.7.2 pH measurement

For the measurement of the pH the pH meter 766 Calimatic of Knick was used. Besides the correct pH adjustment of each equilibration and elution buffer, the pH was recorded during each chromatographic run by the internal ÄKTA device.

3.7.3 UV-Spectroscopy

During the chromatographic runs the UV cell of the ÄKTA Purifier measured continuously the absorption of the liquid phase, containing the protein. The measurement took place at a wavelength of 280 nm. Additionally, each protein solution was measured in a

spectrometer (see Table 3.4). The absorption of the buffers was lower than 0.01 AU and can therefore be neglected.

Table 3.4: The UV absorption of LYS (2 mg/ml), BSA (1 mg/ml) and HCP (0.15 mg/ml) in each buffer at pH 6.5 and 20 mM was measured with the Ultraspec 2100 pro

Buffer	Lysozym E_{280} Spectrometer [AU]	BSA E_{280} Spectrometer [AU]	HCP E_{280} Spectrometer [AU]
Acetate	2.988	0.600	1.341
Bis-Tris	2.988	0.603	1.259
Carbonate	2.987	0.604	1.280
Imidazole	2.986	0.603	1.313
MES	2.986	0.601	1.368
Phosphate	2.986	0.600	1.363

3.7.4 Viscosity

For the measurement of the viscosity of the buffer containing HCPs the Ostwald viscometer was used. Therefore, 3 ml of sample liquid is filled in the right opening of the tube (see Figure 3.5). After that, the viscometer is placed in a temperature bath for at least 10 minutes. Then the liquid is siphoned above the upper line on the left side of the tube. By measuring the flow time of the liquid between the two lines, the kinematic viscosity can be calculated by using equation (3.1) [Schott Instruments].

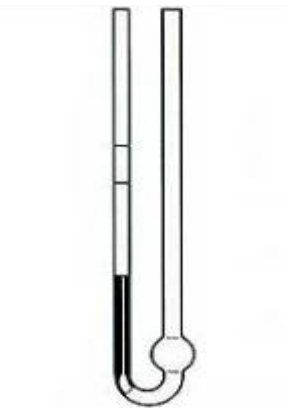

Figure 3.5: Viscometer Ostwald [Schott Instruments].

$$v = K \times t \qquad (3.1)$$

Table 3.5: Viscosity of 20 mM Phosphate, 1 mg/ml BSA, 0.15 mg/ml HCP, K = 0.01

Components	Time [s]	Viscosity [St]
Phosphate	90	0.90
Phosphate + BSA	94	0.94
Phosphate + BSA + HCP	101	1.01

3.7.5 SDS-PAGE

The Sodium dodecyl sulfate-poly acrylamide gel electrophoresis (SDS-PAGE) is a method used for the analysis of proteins and peptides by separating them depending on their molecular weight [Weistermeier & Gronau, 2005]. The method was used for the examination of the purity of the used proteins and protein-protein interactions during zonal chromatography. This SDS-PAGE consisted of two different matrices. A stacking gel, for the concentration of the sample, and a separation gel. The preparation of the SDS-PAGE is listed in Table 3.5. After an hour the polymerization of the gels is complete. They can be used directly or stored with water at 4°C. For the application the sample is mixed 1:1 with sample buffer (see appendix) and boiled at 95°C for 5 min. The setup of the SDS-Page equipment was done by following the manufacturer description (BIO-RAD) and then filled with running buffer (see appendix). The gel pockets were loaded with 5 µl of the marker (Roti®-Mark STANDARD), 15 µl of BSA and Lysozyme (1mg/ml) and 15 µl of each fraction sample. A voltage of 200 V was applied and after one hour the run was complete. As a next step the gels were stained over night by using Coomassie staining (Roti Blue (5x)). Finally, the gels were destained 2 x 30 min with 25% ethanol.

Table 3.6: Composition of the separation and stacking gel for SDS-PAGE sufficient for four gels

Component	Concentration	Separation gel (12 %)	Stacking gel (5 %)
Acryl/ Bisacrylamide	30%	8 ml	3.4 ml
Tris buffer pH = 8.8	3 M	2.5 ml	-
Tris buffer pH = 6.8	1M	-	2.5 ml
SDS	10%	0.2 ml	0.2 ml
VE-H_2O	100%	6.8 ml	11.4 ml
TEMED	100%	10 µl	20 µl
APS	10%	130 µl	130 µl
Cast volume / gel		3.5 ml	1 ml

3.7.6 Bradford protein assay

The Bradford assay is a method for the determination of quantities of proteins at an absorbance of 590 nm. It is often used because of its easy performance, relative sensitivity and specificity for proteins [Zor & Selinger, 1995]. This assay was used for the determination of the HCP concentration.

The dye Coomassie Brilliant Blue-G250 exists in three different condition each absorbing a different wavelength. Through binding to a protein, the dye is transformed from a cationic to an anionic form. This change can be measured at a wavelength of 590 nm and is proportional for a large range of protein concentrations [Roth, 2008]. For the measurement of a protein concentration in microtiter plates a standard dilution series of BSA is necessary. First a stock solution of BSA with a concentration of 400 µg/ml was prepared. Form the stock solution following pipetting scheme was used:

Table 3.7: Dilution series of BSA

BSA [µg/ml]	µl from BSA dilution	H_2O_{dd} [µl]
0	-	110
20	40 µl from 100 µg/ml	160
30	45 µl from 100 µg/ml	105
40	80 µl from 100 µg/ml	120
50	60 µl from 100 µg/ml	60
60	120 µl from 100 µg/ml	80
80	160 µl from 100 µg/ml	40
100	200 µl from 400 µg/ml	600

Then 50 µl of the standard dilution series and the diluted samples were pipetted into the wells of the microtiter plate. For the dye Coomassie Brilliant Blue-G250 solution 2 parts of Roti®-Quant (5x) and 5.5 parts of H_2O_{dd} were mixed. 200 µl of this solution were then added to each standard and sample well. After an incubation time of 5 min at room temperature, the microtiter plate can be placed inside the MULTISKAN (Thermo) and is ready to be measured. For the evaluation, the OD was plotted against the protein concentration (see Figure 3.6).

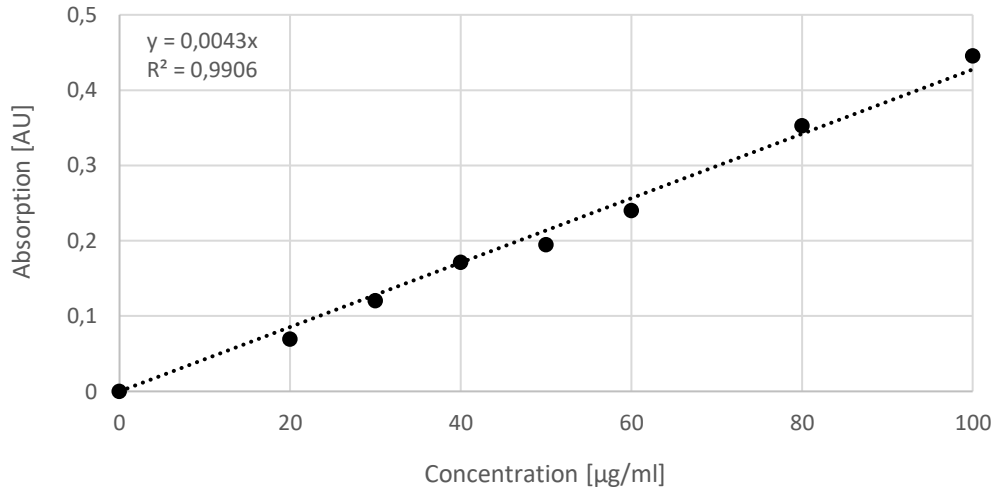

Figure 3.6: Calibration curve of the dilution series of BSA after subtraction of the blank value

Based on the y-value of this standard straight line, it is possible to calculate the protein concentration of the sample solution. For the determination of the protein concentration from the cell disruption five different dilutions were prepared and measured (see Table 3.7). The final host cell protein concentration was 7.045 mg/ml.

Table 3.8: Determination of the host cell protein concentration of the disrupted E. coli suspension using five different dilutions and y= 0.0043x

Dilution	UV-absorption [AU]	Concentration [mg/ml]
1:20	1.416	6.486
1:40	0.744	6.921
1:50	0.589	6.849
1:80	0.376	6.996
1:100	0.305	7.093
		7.0445

4. Results and Discussion

In the following chapter the results of the zonal and frontal chromatography of BSA, lysozyme and HCP will be presented and discussed. First, the results of the zonal chromatography will be presented to get an understanding of the protein-protein interactions. Thereupon, the frontal chromatographic runs will be analyzed by means of dynamic and static binding capacities. The first experiments were performed under the same pH (6.5) and salt concentrations (20 mM). In additional experiments either the pH or the salt concentration was changed. Both an anion and a cation exchanger were used. The flow rate of 1 ml/min remained constant over all chromatographic experiments.

4.1 BSA and Lysozyme

Purity of BSA and Lysozyme

Before starting with the test series, the purity of the BSA (IgG free, Roth) and lysozyme (Sigma-Aldrich) was examined regarding the necessity of washing steps. For this a SDS-PAGE was performed with three different concentrations of lysozyme (1,2 and 3 mg/ml) and a reducing and a non-reducing sample of BSA (1 mg/ml). The results can be seen in Figure 4.1. With increasing lysozyme concentration three additional bands can be identified clearly. The first one is between 66 and 118 kDa, the second around 29 kDa and the third band is located between 14 and 20 kDa. The most intense band at 14 kDa fits the molecular weight of lysozyme.

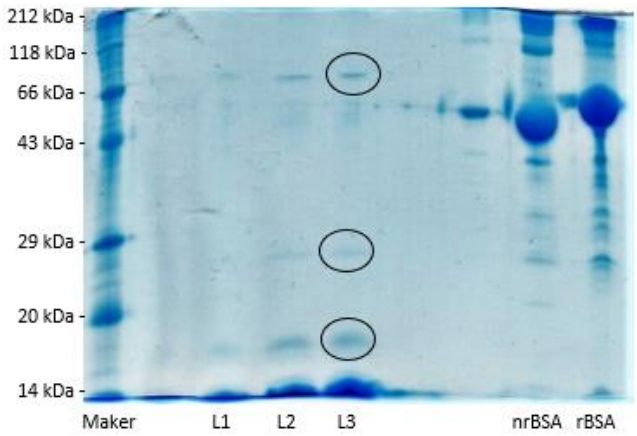

Figure 4.1: SDS-Page of lysozyme (1,2 & 3 mg/ml) and BSA (1 mg/ml).

Note. L = lysozyme. nr = non-reducing. r = reducing.

Table 4.1 shows the composition of proteins which are present in chicken egg white as well as the abundance, their molecular weight and the pI. By comparing the table with the SDS-PAGE, the first two bands could be caused by Ovotransferrin (76 kDa) and Ovomucoid (28 kDa). Due to their pI, they are negatively charged at a pH of 6.5 und thus will not bind to the cation exchanger. [Gossett, Rizvi & Baker, 1984].

Table 4.1: Compositions of proteins in hen egg white [Gossett et al., 2013]

Protein	Abundance [%]	Molecular weight [kDa]	pI
Ovalbumin	54	44	4.5
Ovotransferrin	12	76	6.1
Ovomucoid	11	28	4.1
Ovoglobulin G2/G3	4/4	36/45	4.8/5.5
Ovomucin	3.5	110	4.5-5.0
Lysozyme	3.4	14.3	11.35
Ovoglycoprotein	1	24	3.9
Avidin	0.05	66	10
Cystatin	0.05	13.3	-

By looking at the bands of the non-reducing and reducing sample of BSA significantly more impurities can be observed above and below the actual BSA band at 66 kDa compared to lysozyme. The reduced sample of BSA shows a higher molecular weight due to the stronger unfolding of BSA. Table 4.2 shows possible additional proteins which can be found in blood plasma. The bands above 66 kDa could also be agglomerates of BSA molecules [Rösch et al., 2016]. As in the product description of BSA (Roth), IgG shouldn´t be present.

Table 4.2: Molecular weight and pI of proteins in human blood plasma [Mohan, 2006]

Protein	Molecular weight [kDa]	pI
Albumin	66	5.2
Alpha 1 globulins	93	-
Ceruloplasmin	135	4.4
C-reactive protein	110	4.8
Fibrinogen	340	5.5
IgG	150	6-8
Plasmin	83	7-8.5
Transferrin	80	5.9
Thrombin	36	7.1

The results of the SDS-PAGE suggest that BSA, in combination with the anion exchanger, will lead to a stronger contamination of the column. Therefore, a more frequent cleaning

step with NaOH must be performed compared to the cation exchanger CM FF (see chapter 3.6).

4.1.1 Anion exchanger

Zonal chromatography

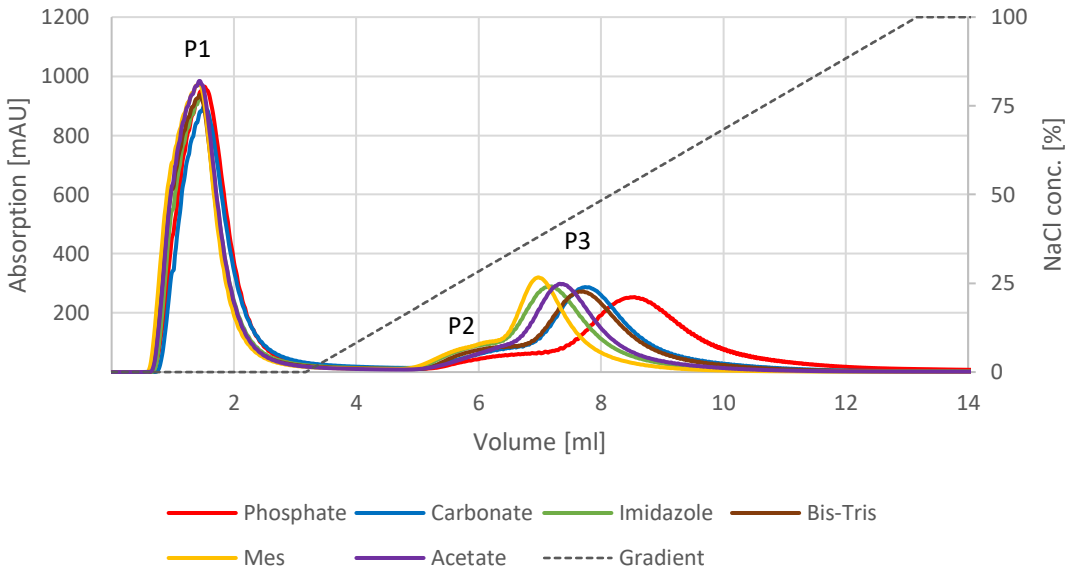

Figure 4.2: Zonal chromatography of BSA (1 mg/ml) and LYS (1 mg/ml) at a pH of 6.5. Flow rate = 1 ml/min. Buffer A = 20 mM. Buffer B = 1 M NaCl. Gradient time = 10 CV. Column = DEAE.

The zonal chromatography was performed to examine the binding of BSA in the present of lysozyme to the DEAE column using different buffer solutions. Therefore, a sample of 1 ml containing 1 mg/ml BSA and 1 mg/ml LYS were applied in the present of 20 mM buffer. After a gradient delay of 2 CV, which is used to wash out unbound protein, the linear gradient begins. After 10 CV 100% Buffer B is reached and all bound protein should be eluted. This process is displayed in Figure 4.2. The first peak should be caused by the positively charged lysozyme which cannot bind to the anion exchanger. The second peak is in fact a double peak leading to the assumption that besides BSA, a certain amount of lysozyme was able to bind to the column, too. For the conformation of this assumption a SDS-PAGE was performed (see Figure 4.3). The first lane contains the marker (Roth) and the other three lanes the samples. The SDS-PAGE shows that in the first peak (P1) solely lysozyme is present (single band at 14 kDa). In the P2 sample a lysozyme band and a weak BSA (66 kDa) band can be identified. For the third peak the amount of BSA is significantly great and there is also a distinct lysozyme band present. This suggests that LYS^+ and BSA^- form a complex due to their opposite charge. Because BSA has a 5 x greater molecular

mass as lysozyme, it is possible that BSA interacts with more than one lysozyme molecule at a time when forming an ionic complex. This could explain why the amount of lysozyme is greater in the third peak than in the second. The interaction between LYS^+ and BSA^- can either happen in the protein solution or at the column matrix. The reasons could be that first BSA is adsorbed onto the surface and then lysozyme molecules can bind to the adsorbed BSA. This behaviour has already been studied by Rösch et al. (2016). They examined the cooperative adsorption of different BSA and LYS ratios after incubation on dental titanium samples and the formation of agglomerates of BSA and LYS ratios by applying fast protein liquid chromatography and an anion exchanger. They also observed three fractions with the anion exchanger. The first on containing only lysozyme and the second and third fraction containing BSA and LYS.

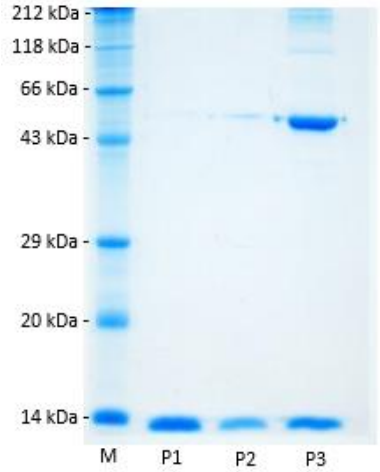

Figure 4.3: SDS-PAGE of the zonal peaks from the DEAE column.

Note. M = Protein standards. P = Peak.

Besides the SDS-PAGE, the area of each peak was determined. The calculated values are presented in Table 4.3:

Table 4.3: BSA/LYS peak areas from zonal chromatography (20 mM)

Buffer	Peak area [AV]		
	P1	P2	P3
Phosphate	940.06	87.19	424.59
Acetate	938.75	85.47	418.35
MES	926.28	88.77	420.71
Imidazole	893.65	99.23	410.73
Bis-Tris	890.13	105.64	409.30
Carbonate	891.21	102.53	413.25

Note. P = Peak

By looking at the individual peak areas of each buffer, differences in UV-absorption can be determined. The peak areas can be divided into two groups. The first group comprises the buffers phosphate, MES and acetate. Their first peak area is above 920 AV whereas the areas for carbonate, imidazole and Bis-Tris is around 890 AV. This grouping can also be observed on the second peak. The second group shows an area for the middle peak of around 100 AV. Concerning the first group, the area of the second peak is smaller. The area of the third peak is almost similar for all buffers. Therefore, it seems likely that carbonate, imidazole and Bis-Tris enable a better interaction of lysozyme with the column, maybe by the mediator BSA

Frontal chromatography of BSA

Before the influence of lysozyme on BSA during frontal chromatography can be evaluated, "blank" runs of solely BSA with a concentration of 1 mg/ml at pH of 6.5 and a buffer salt concentration of 20 mM have been performed. The results can be seen in Figure 4.4.

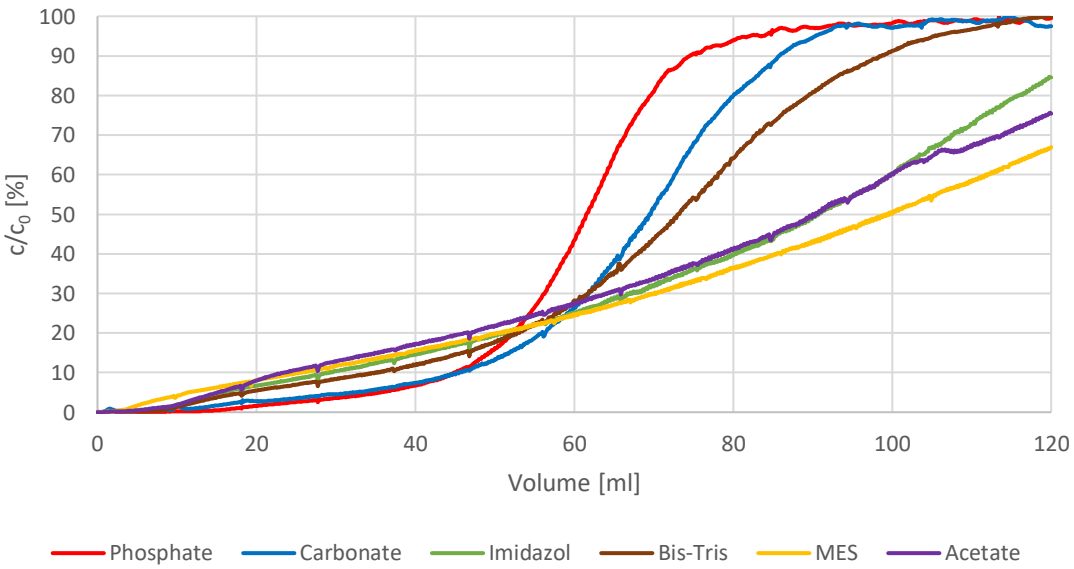

Figure 4.4: Frontal chromatography of BSA (1 mg/ml). Flow rate = 1 ml/min. Buffer concentration = 20 mM. pH = 6.5. Column = DEAE.

The six received breakthrough curves all differ from each other regarding the curve shape and binding capacity. The buffers phosphate, carbonate and Bis-Tris meet the typical S-form of a breakthrough curve whereas, imidazole, MES and acetate can´t reach a plateau within the 120 minutes of sample application. Hence, the SBC can only be calculated for phosphate, carbonate and Bis-Tris. When looking at the point at which 10% breakthrough is reached, phosphate and carbonate show the latest breakthrough followed by Bis-Tris

and imidazole. MES and acetate are the two worst performing buffers. The exact values are presented in Table 4.4. Additionally, the molecular mass, the share of charged ions and the conductivity of each buffer is listed in that table. *Herrmann* (2002) and *Niu* (2015) assumed, that buffer salt ions which carry the same charge as the protein compete for binding sites or change the zeta potential of the stationary phase, respectively. Thus, the adsorption of the protein is slowed down or prevented. On the other hand, oppositely charged salt ions should support the binding of the protein by attaching to the adsorbed protein, overlaying its negative charge and enable the built-up of another protein layer. Both effects are enhanced by multivalent ions. These so-called salt effects are nonspecific and should be independent of the used salt type [Tsumoto et al., 2006]. In case of the static binding capacity a correlation can be found. Bis-Tris, as a positively charged buffer salt, is approaching the highest SBC, followed by carbonate (monovalent anions). Phosphate, composted of mono (16.67 mM) - and divalent (3.33 mM) anions, has the lowest SBC. The question arises, why acetate, imidazole and MES lead to an incomplete breakthrough curve within the 120 ml. An explanation for imidazole could be that due to its higher pK_A value compared to Bis-Tris (6.95 vs. 6.46) the share of monovalent cations is greater. Instead of enhancing the absorption of BSA to the stationary phase by building-up another protein layer, imidazole molecules may already “bind” to the protein in solution and thereby shielding the negative charge of BSA and thereby inhibiting its binding to the column. Due to the smaller size of imidazole compared to Bis-Tris, more salt ions should be able to attach to BSA in a shorter time. This effect could also explain the lower $DBC_{10\%}$ of imidazole compared to Bis-Tris. The negative effect of acetate on the breakthrough curve could be explained by its high ionic strength at pH 6.5. Due to the low pK_A value of 4.76, 19.64 mM of the ions are negatively charged. *Shi et al.* (2005) have shown in their batch experiments with BSA that an increasing ionic strength leads to lower attraction between the protein and the stationary phase. MES however, doesn´t seem to fit into this concept. Even though the concentration of charged ions is lower than the one of phosphate, the breakthrough curve is not completed and the $DBC_{10\%}$ is the second lowest. In comparison to all negatively charged buffers, MES has the lowest conductivity (1.02 mS/cm). Also, MES is the only zwitterion in these experiments. This could also have an impact on the protein-adsorber interactions.

Table 4.4: Characteristics, $DBC_{10\%}$ and SBC of all buffers

Buffer	Molecular mass [g/mol]	Charge [mM]	Conductivity [mS/cm]	$DBC_{10\%}$ [mg/ml]	SBC [mg/ml]
Carbonate	105.99	- 11.71	3.35	45.50	67.19
Phosphate	156.01	- 16.67/ -- 3.33	2.16	44.93	60.91
Bis-Tris	209.24	+ 9.54	0.54	34.93	70.03
Imidazole	68.08	+ 14.76	1.34	29.20	-*
MES	195.20	- 14.31	1.02	25.33	-*
Acetate	136.08	- 19.64	1.80	23.47	-*

Note. *SBC cannot be calculated due to incomplete breakthrough curve. - : monovalent anions. -- : divalent anions. + : monovalent cations.

By looking at the dynamic binding capacity of the buffers it stands out that the order of the $DBC_{10\%}$ is not in accordance with the SBC. Bis-Tris has the highest SBC with 70.03 mg/ml, but regarding the DBC is ranked third. *Skidmore, Horstmann & Chase* (1989) suggest that at the beginning of the sample application the diffusion paths are shorter, because the adsorption takes place only in the outer region of the stationary phase. Therefore, the adsorption is faster compared to the later phase where BSA molecules must be adsorbed deeper into the pores. It appears that during the first part of the breakthrough curve (from which the DBC is calculated), other factors seem to have a stronger influence on the binding capacity than towards the end of the frontal chromatography. In case of BSA the two negatively charged buffers with the highest conductivity achieve the best results for the dynamic binding capacity. Only then to be followed by the two positively charged buffers Bis-Tris and imidazole. This suggests that the shielding effect of the cations has a more negative influence on the protein adsorption than competitive adsorption of salt ions. This effect could also be influenced by the fact that the cations were able to interact with BSA in the protein solution before being applied on the column. Regarding acetate it looks like exceeding a certain limit of ionic strength is exceeded it has a negative impact. The low conductivity of MES might be unfavorable, too. It must also be considered that BSA forms dimers in solution. *Skidmore et al.* (1989) have found out that the share of dimers was higher in the eluate than in the fresh protein solution. The formation of dimers may lead to a higher binding capacity due to the effect that BSA molecules bind to already adsorbed molecules, creating a “double layer” of BSA. Double layer means that protein is adsorbed in several layers [Herrmann, 2002]. Results of the Bachelor thesis of *Mashhori Ghaleh*

Babakhani (2017) showed that the share of dimers is the highest with carbonate and phosphate.

Frontal chromatography of BSA/LYS

For the next experiments a protein solution of 1 mg/ml BSA and 1 mg/ml lysozyme was prepared and applied on the anion exchanger. Figure 4.5 shows the frontal chromatogram of this protein mixture.

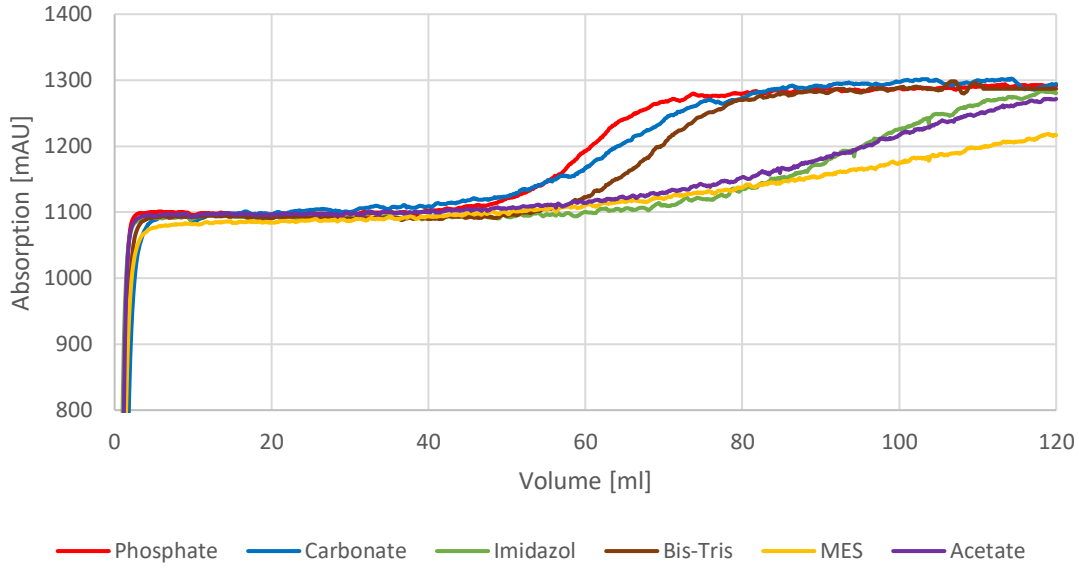

Figure 4.5: Frontal chromatography of BSA (1 mg/ml) and LYS (1 mg/ml). Flow rate = 1 ml/min. Buffer concentration = 20 mM. pH = 6.5. Column = DEAE.

It can be seen, that an immediate breakthrough of lysozyme occurs. This is caused by the repulsion of lysozyme and the column (both are positively charged). After a plateau is attained at about 1100 mAU, a second breakthrough curve appears caused by BSA. On first examination, differences to the pure BSA breakthrough curve can be noticed. The first part of the curve is flatter, and the 10% breakthrough has shifted to the right for most buffers. For a better comparability of both runs, the BSA/LYS curve is set to a corrected baseline. For this, the adsorption of the lysozyme plateau is subtracted, and the obtained value equals the new baseline. Thereupon, the breakthrough curves are normalized by the maximum absorption of each curve. The results are presented in Figure 4.6.

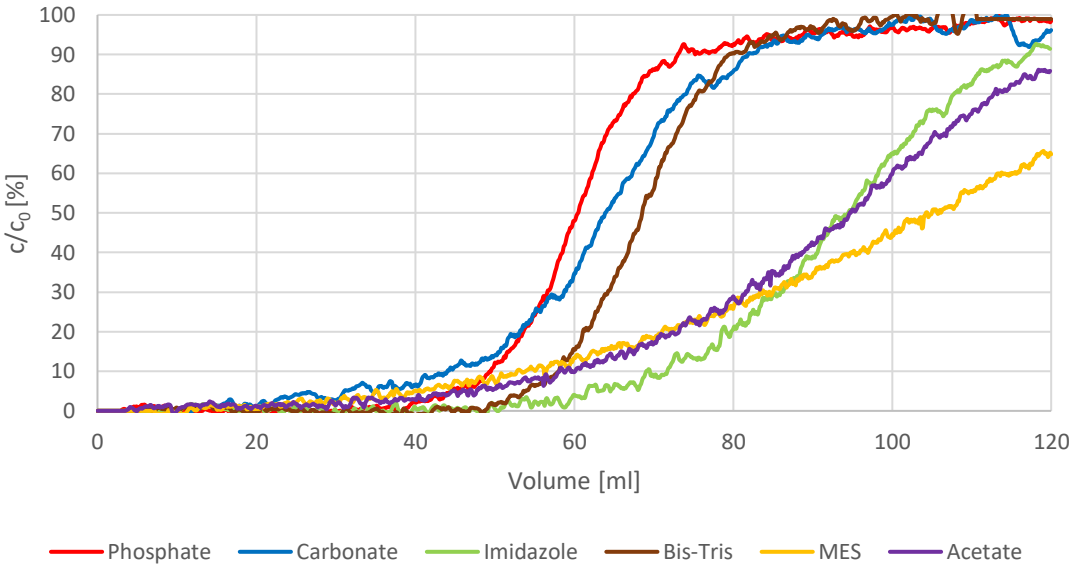

Figure 4.6: Frontal chromatography of BSA (1 mg/ml) and LYS (1 mg/ml) with corrected baseline. Flow rate = 1 ml/min. Buffer concentration = 20 mM. pH = 6.5. Column = DEAE.

While the breakthrough curve (BTC) of phosphate and carbonate remain almost unchanged compared the BSA experiments, significant differences regarding the other four buffers can be noted. The breakthrough of Bis-Tris is steeper and resembles more strongly the typical sigmoidal form of a BTC. For the buffers acetate, imidazole and MES the course of the BTC remains incomplete, but the curves are closer to the baseline, so that less protein is waster during the first part of the breakthrough. For the calculation of the DBC and SBC a protein concentration of 1 mg/ml was assumed because most of lysozyme dose not bind to the column. The corresponding values are presented in Table 4.5. The SBC has slightly deteriorated for Bis-Tris and carbonate whereas, for phosphate the value has slightly improved. The differences in the $DBC_{10\%}$ are far greater. The buffer ranking has almost reversed. With a $DBC_{10\%}$ of 44.09 mg/ml for carbonate, the value has even changed for the worse. Whereas, the other buffers all show an improvement, particularly acetate, imidazole and MES. Their $DBC_{10\%}$ has more than doubled (see Table 4.6). *Palacio, Ho, Prádanos, Hernández and Zydney* (2003) have shown in their work that lysozyme increases the zeta potential of BSA to a less negative value. Therefore, positively charged buffer ions may not be attracted to the BSA molecule as much as in the pure BSA solution, having a lesser impact on the protein adsorption and thus, resulting in an improved binding capacity. Another aspect which has to be considered is that BSA molecules have a repulsive effect among themselves [Meissner, Prause, Bharti &

Findenegg, 2015]. This repulsion should be higher in the presence of anions and lower with cations. Through the interaction of BSA^- and $lysozyme^+$ the impact of buffer salt ions, regarding this mechanism, is maybe lowered.

Table 4.5: $DBC_{10\%}$ and SBC of the frontal chromatography of BSA/LYS on a DEAE column

Buffer	$DBC_{10\%}$ [mg/ml]	SBC [mg/ml]
Imidazole	69.70	-*
Acetate	58.15	-*
Bis-Tris	58.03	69.09
MES	52.80	-*
Phosphate	49.54	62.19
Carbonate	44.09	64.14

Note. *SBC cannot be calculated due to incomplete BTC.

This could explain the improvement of acetate (+ 147 %). At pH 6.5 acetate has the greatest share of anions and therefore, decreasing the zeta potential of BSA which leads to a strong repulsion between the BSA. Consequently, BSA molecules interfere with themselves during adsorption. Lysozyme seems to be weakening this effect. This might also enable the build-up of multiple protein layers consisting out of BSA and LYS molecules, increasing the number of proteins which can be adsorbed and thereby, the dynamic binding capacity. The same assumption could be applied with MES. Regarding carbonate and phosphate, their influence on the adsorption appear to be less pronounced, having neither a strong positive nor negative impact.

Table 4.6: Comparison of the $DBC_{10\%}$ of BSA and BSA/LYS

Buffer	$DBC_{10\%}$ of BSA [mg/ml]	$DBC_{10\%}$ of BSA/LYS [mg/ml]	Percentage [%]
Carbonate	45.50	44.09	- 3.10
Phosphate	44.93	49.54	+ 10.26
Bis-Tris	34.93	58.03	+ 66.13
Imidazol	29.20	69.70	+ 138.7
MES	25.33	52.80	+ 108.4
Acetate	23.47	58.15	+ 147.8

4.1.2 Cation exchanger

Zonal chromatography

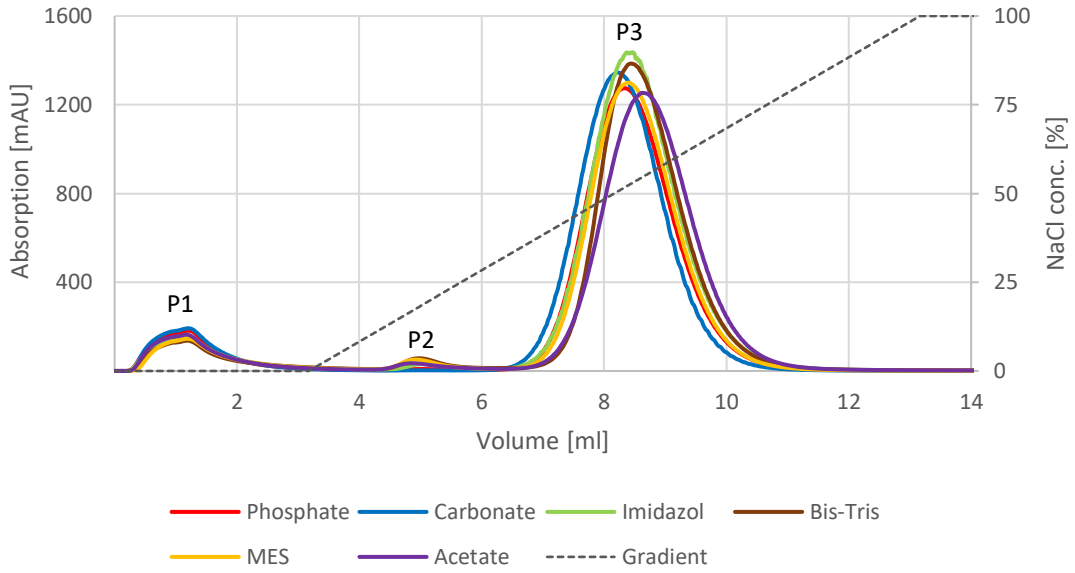

Figure 4.7 Zonal chromatography of LYS (2 mg/ml) and BSA (1 mg/ml). Flow rate = 1 ml/min. Buffer A = 20 mM. Buffer B = 1 M NaCl. pH = 6.5. Gradient time = 10 CV. Column = CM.

As with the anion exchanger, a zonal chromatography was performed with the cation exchanger in the present of lysozyme, BSA and a buffer. Again three peaks can be observed (see Figure 4.7). The first peak is probably the washed out BSA which cannot bind to the column due to its charge. The small second peak could be a combination of BSA and lysozyme and the third peak is the lysozyme peak. For a more accurate statemant a SDS-PAGE was performed (see Figure 4.8). Besides the three peak samples, a sample from the stock solution was apllied (second lane). In the stock solution the BSA and lysozyme band can be clearly identified as well as some agglomerates. P1 shows the strongest band for BSA and a light band of lysozyme. In the sample from the second peak (P2) a weaker BSA and a slightly stronger lysozyme band can be seen. In the third sample (P3) only lysozyme can be detected. The lower proportion or absence of BSA in the second and third peak may be due to the fact that lysozyme is significantly smaller than BSA (14,3 kDa compared to 66.2 kDa). This should also be reflected in the size of the peak area which are presented in the table below.

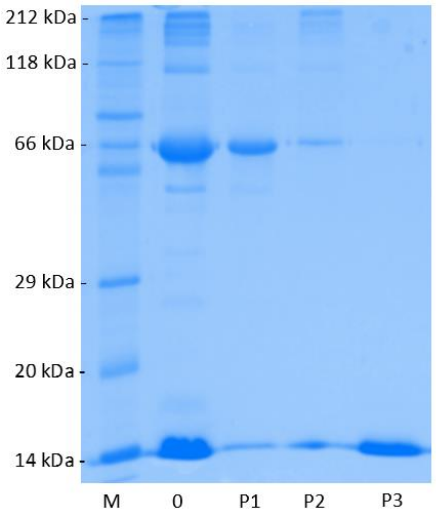

Figure 4.8: SDS-PAGE of the zonal peaks, CM column.

Note. M = Protein standards. P = Peak. 0 = stock solution.

Table 4.7 shows that there is a shift of the peak area size from the first to the second and third peak in the order of carbonate to Bis-Tris. Carbonate produces the largest first peak area (252.03 AV) and the smallest second and third area (4.44 and 2170.27 AV) whereas Bis-Tris peak areas shift to 195.95 AV, 56.26 and 2212.26 AV. Taking that in account, it can be assumed that in the presence of a negatively charged buffer salts more lysozyme can bind to BSA leading to a larger first peak. On the other hand, positively charged buffer salts may shield the negative charge of BSA and thus more lysozyme can bind to the column directly. At the same time this shielding effect may enable the binding of BSA to the column. Different studies, e.g. *Skidmore et al.* (1989), have also stated that BSA is able to bind onto cation exchanger at pH at which the net charge of BSA should be negative. They assumed an asymetrical charge distirubution, so that one reagion carries a positive charge which enables binding to the cation exchanger.

Table 4.7: LYS/BSA peak areas from zonal chromatography of each buffer (20 mM)

Buffer	Peak areas [AV]		
	P1	P2	P3
Carbonate	252.03	4.44	2170.27
Phosphate	240.95	9.82	2188.28
Acetate	225.73	36.51	2191.36
Imidazole	224.36	32.29	2181.02
MES	205.78	52.38	2193.33
Bis-Tris	195.95	56.26	2212.26

Note. P = Peak

Frontal chromatography of LYS

As with BSA, “blank” runs were performed with lysozyme. The protein concentration was 2 mg/ml. The buffers had a pH of 6.5 and a salt concentration of 20 mM. The corresponding breakthrough curves are shown in Figure 4.9.

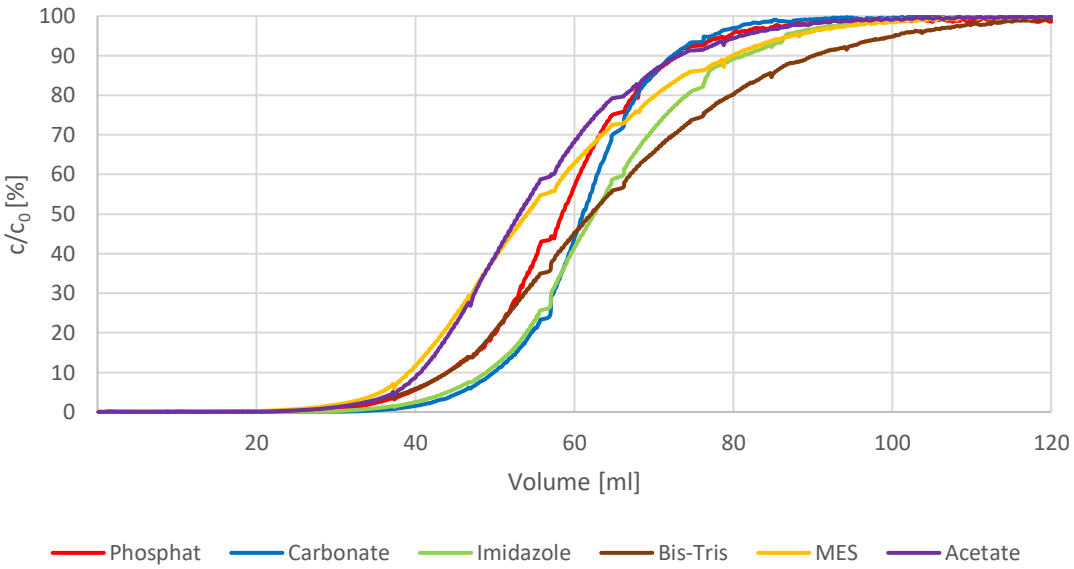

Figure 4.9: Frontal chromatography of LYS (2 mg/ml). Flow rate = 1 ml/min. Buffer concentration = 20 mM. pH = 6.5. Column = CM.

All six received breakthrough curves show a sigmoidal form. The first part of the curves (0 – 30 ml) is significantly closer to the x-axis than the curves of BSA with the anion exchanger. The steepness of the curves is also more distinctive. Overall, this indicates a better binding capacity of lysozyme compared to BSA which could be explained by the considerably smaller size of lysozyme (14.3 kDa ↔ 66.2 kDa). More lysozyme molecules can fit onto the surface area of the stationary phase and they are also able to penetrate pores which are too restricted for BSA [Skidmore et al., 1989]. The best breakthrough curve has lysozyme in combination with the carbonate buffer, followed by imidazole. Phosphate and Bis-Tris start off similar, however at an applied volume of about 53 ml, the two curves separate, leading to a similar $DBC_{10\%}$ but different SBC (see Table 4.8). Another pair is formed by acetate and MES. They have the worst values for the $DBC_{10\%}$ and SBC. The largest amount of protein which could be bound to the column, is in the presence of both positively charged buffers (Bis-Tris and imidazole) which is surprising since it is assumed that they would compete with lysozyme for binding sites on the stationary phase. In the case of lysozyme, it must be considered that due to the pH of 6.5 and the pI of 11.35 LYS is strong

positively charged. For this reason, the negatively charged buffer salt ions are attracted more strongly to the protein, leading to more effective shielding and thereby, lowering the zeta potential of lysozyme to a level that deteriorates the static binding capacity. This effect seems to have a more negative influence on the SBC than competitive binding of the cations to the column. This could explain the better performance of the positively charged buffers. *Faude, Zacker, Müller and Böttinger* (2007) investigated the influence of the buffer concentration on the DBC of human monoclonal antibodies. They observed that a higher ionic strength of a buffer leads to a lowering of the zeta potential of the antibody. And a lower zeta potential reduces the affinity of the protein to the stationary phase. This could explain the outcome for the buffers carbonate, phosphate and acetate. Again, MES leads to a lower SBC than phosphate even though its ionic strength is lower.

Table 4.8: Characteristics, $DBC_{10\%}$ and SBC of all buffers

Buffer	Molecular mass [g/mol]	Charge [mM]	Conductivity [mS/cm]	$DBC_{10\%}$ [mg/ml]	SBC [mg/ml]
Carbonate	105.99	- 11.71	3.35	99.70	122.44
Imidazole	68.08	+ 14.76	1.34	97.60	127.54
Phosphate	156.01	- 16.67/-- 3.33	2.16	87.92	117.46
Bis-Tris	209.24	+ 9.54	0.54	87.84	129.52
Acetate	136.08	- 19.64	1.80	81.06	110.66
MES	195.20	- 14.31	1.02	78.28	113.90

Note. - : monovalent anions. -- : divalent anions. + : monovalent cations.

Concerning the dynamic binding capacity, a different ranking of the buffers is obtained compared to the SBC. As described earlier, carbonate (11.71 mM anions) and imidazole (14.76 mM cations) have the best DBC with 99.7 and 97.6 mg/ml followed by phosphate (16.67/3.33 mM mono-/divalent anions) which almost has the same dynamic binding capacity as Bis-Tris (9.54 mM cations), both about 88 mg/ml. At the bottom of the table are acetate (19.64 mM anions) and MES (14.31 mM anions) with a DBC of around 80 mg/ml. Unlike BSA, no distinct order regarding the buffer type or ionic strength can be made. One explanation could be the size of lysozyme. As mentioned before, lysozyme can be adsorbed faster and more efficient because of its small size. Because of the strong positive net charge of lysozyme carbonate with the smallest share of anions should have the least impact on the zeta potential. With increasing number of anions this shielding effect gets stronger, resulting in a lower binding capacity. Regarding the cations of imidazole and Bis-

Tris, the competition for adsorption sites seems to have a minor influence on the dynamic binding capacity than the shielding. Whereby, the smaller size and higher ionic strength of imidazole appears to be more favorable than the attributes of Bis-Tris. The relation of the shielding effect to the completive binding is similar to the results achieved with BSA and the anion exchanger.

Frontal chromatography of LYS/BSA

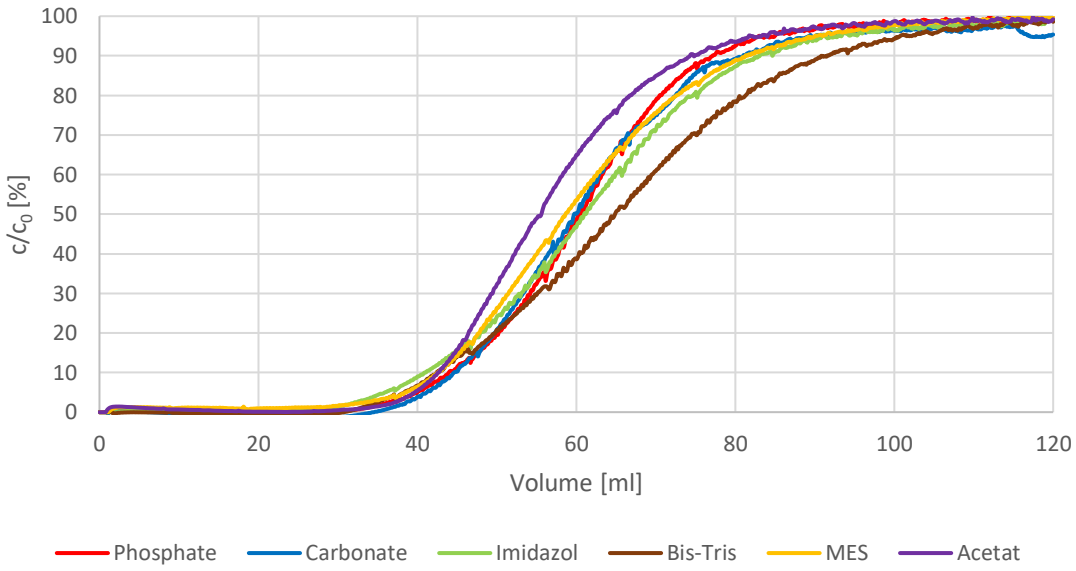

Figure 4.10: Frontal chromatography of lysozyme (2 mg/ml) and BSA (1 mg/ml) with corrected baseline. Flow rate = 1 ml/min. Buffer concentration = 20 mM. pH = 6.5. Column = CM.

Figure 4.10 shows the results of the frontal chromatographic runs when 1 mg/ml BSA is added to the 2 mg/ml lysozyme protein solution. In contrast to the experiments with only lysozyme, a bundling of the curves can be recognized. The range of the $DBC_{10\%}$ of all six buffers is significantly smaller. The difference between the best and worst DBC is only 7 mg/ml (see Table 4.9). By the application of solely lysozyme the range was 20 mg/ml. In general, it can be said that the influence of BSA on the binding capacity of lysozyme is less pronounced than the other way around. This becomes apparent by looking at Table 4.10. The change of the $DBC_{10\%}$ only varies around plus/minus 15 %. With the anion exchanger an increase of 150 % could be observed. Regarding the SBC, the changes are even minor (± 4 mg/ml).

Table 4.9: $DBC_{10\%}$ and SBC of the frontal chromatography of LYS/BSA on a CM column

Buffer	$DBC_{10\%}$ [mg/ml]	SBC [mg/ml]
Carbonate	89.34	125.06
Phosphate	87.94	122.34
MES	85.50	120.88
Acetate	85.34	114.78
Bis-Tris	85.06	132.98
Imidazole	82.14	124.34

What stands out is the decrease of the dynamic binding capacity of carbonate and imidazole. Just as lysozyme increases the zeta potential of BSA, BSA should also have an influence on the zeta potential of lysozyme. This should result in a less positively charged molecule, weakening the negative buffer effects of acetate and MES. Imidazole could hinder the interaction of BSA to lysozyme and the column and thereby reduce the number of adsorption sites for lysozyme. *Skidmore et al.* (1989) mention in their paper, that BSA is able to bind to more than one adsorption site at a time. Imidazole (and also Bis-Tris) could shield the negative charge of BSA and thus a formation of a protein layer on the column is reduced. According to the assumption made above, carbonate should lead to a decrease of the dynamic binding capacity (-10.39 %).

Table 4.10: Comparison of the percentage $DBC_{10\%}$ between LYS and LYS/BSA

Buffer	$DBC_{10\%}$ of LYS [mg/ml]	$DBC_{10\%}$ of LYS/BSA [mg/ml]	Percentage [%]
Carbonate	99.70	89.34	- 10.39
Imidazol	97.60	82.14	- 15.84
Phosphate	87.92	87.94	+ 0.02
Bis-Tris	87.84	85.06	- 3.16
Acetate	81.06	85.34	+ 5.28
MES	78.28	85.50	+ 9.22

Regarding to the course of the pH (see Figure 4.11) it can be seen that the pH doesn´t remain constant, but slowly increases over time. In the presents of BSA, carbonate, having the lowest share of monovalent anions (11.71 mM), seems to be weakened in its buffer capacity. This could be the factor which is responsible for the worsening the DBC in carbonate buffer.

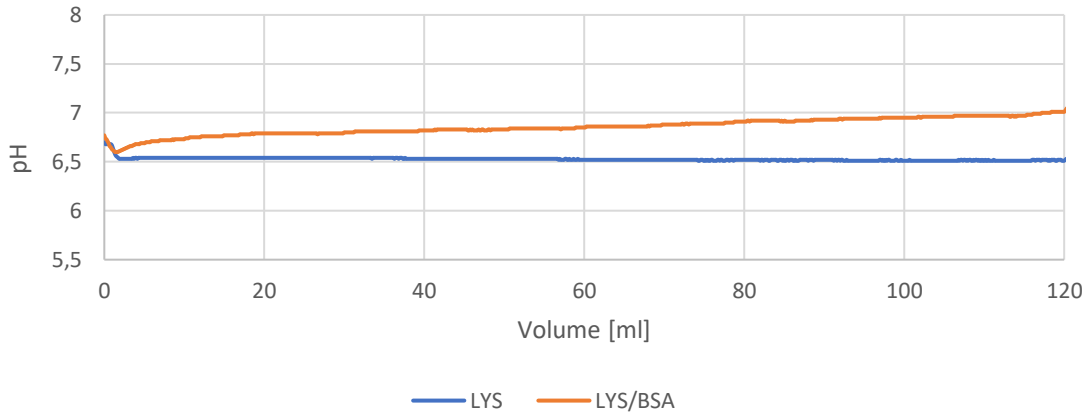

Figure 4.11: pH value curves during frontal chromatography of lysozyme and BSA/LYS. Flow rate = 1 ml/min. Buffer concentration = 20 mM carbonate. pH = 6.5. Column = CM.

4.2 Host cell proteins

4.2.1 Anion exchanger

Determination of the HCP concentration

For the experiments with HCPs and BSA it was necessary to determine in advance the required concentration of HCPs. This concentration should be chosen so that the zonal peak areas of both proteins are approximately equal. The zonal peak area of 1 mg/ml BSA is on average 334.22 AV.

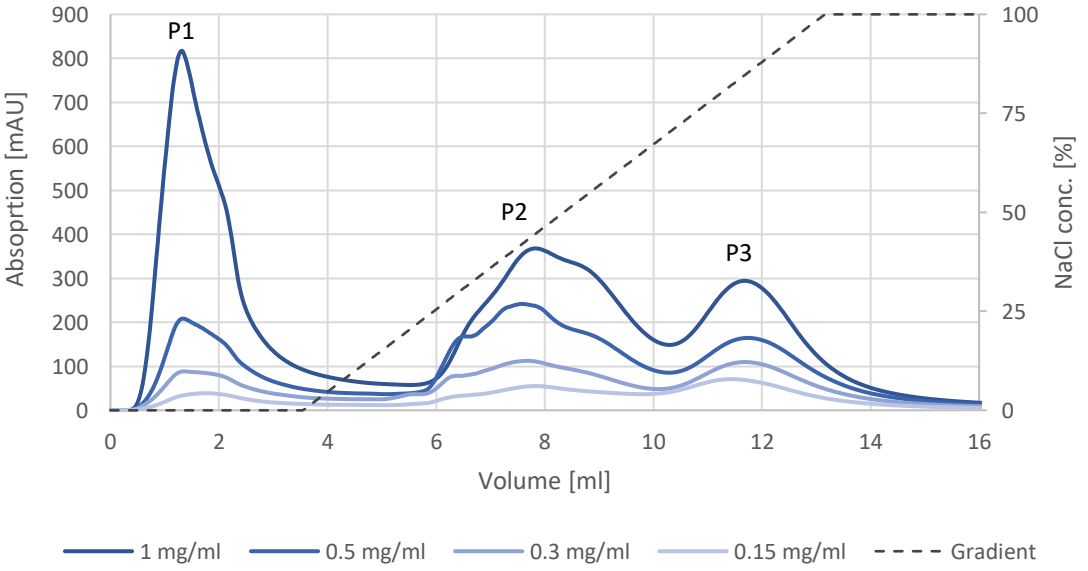

Figure 4.12: Chromatogram of different HCP concentrations. Injection of 1 ml sample with 0.15, 0.3, 0.5 and 1 mg/ml HCP concentration at pH 6.5. Flow rate = 1 ml/min. Buffer A = 20 mM phosphate. Buffer B = 1 M NaCl. Column = DEAE. P = Peak.

Therefore, different HCP concentration were applied manually on the DEAE column via a 1 ml sample loop. As the equilibration buffer phosphate with a concentration of 20 mM was chosen. The elution buffer has an additional salt concentration of 1 M NaCl. This method is designed to run like the zonal chromatography method. For the first test run a HCP concentration of 1 mg/ml was applied. As is can be seen in Figure 4.12 and Table 4.11 three peaks appear. The total peak area of this concentration is by far greater than of BSA. In a first step the HCP concentration was halved to 0.5 mg/ml. Still the total peak area is four times greater as of 1 mg/ml BSA. A further reduction to 0.3 mg/ml leads to an approach of the desired value. Due to linearity of the adsorption the HCP concentration is again halved to 0.15 mg/ml. This leads to a total peak area of 381.77 AV which approximately equals to the peak area of BSA. Therefore, this concentration will be used in the experiments concerning BSA and HCPs.

Table 4.11: Peak areas of different HCP concentrations at pH 6.5 and 20 mM phosphate

Concentration [mg/ml]	Peak 1 [AV]	Peak 2 [AV]	Peak 3 [AV]	Total peak area [AV]
1	1074.06	956.05	661.44	2691.75
0.5	344.22	637.65	409.79	1391.66
0.3	174.71	318.67	278.13	771.51
0.15	79.54	125.93	176.30	381.77

Zonal chromatography

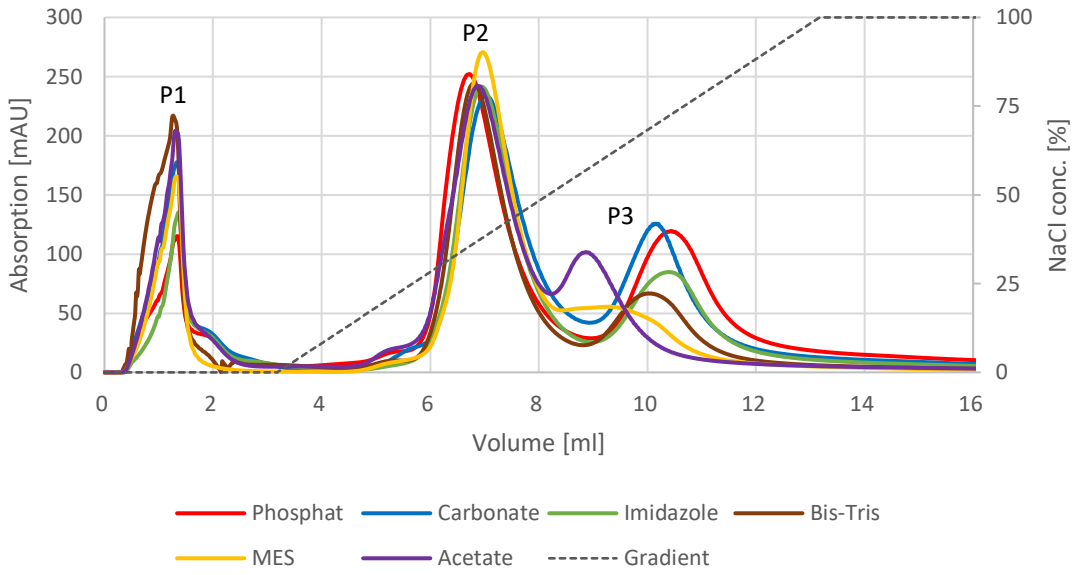

Figure 4.13: Zonal chromatography of BSA (1 mg/ml) and HCP (0.15 mg/ml) at a pH of 6.5. Flow rate = 1 ml/min. Buffer A =20 mM. Buffer B = 1 M NaCl. Gradient time = 10 CV. Column = DEAE.

Like in the other zonal chromatograms three peaks can be identified (see Figure 4.13). This time the first and third peak's height and form varies greatly among each buffer. The first peak assumingly contains the positively charged HCPs whereas, the other two peaks include BSA and the negatively charged HCPs. For a closer look on the composition of each peak a SDS-PAGE was carried out. The results of the gel electrophoresis are shown in Figure 4.14. The first lane contains the marker (Roth) and the second lane a 1:10 diluted probe of HCPs. The pockets 3 to 5 were loaded with the peak samples. In the HCP sample multiple proteins with different molecular masses can be identified. Two bands stand out. The first band is placed between the 29 kDa and 43 kDa marker and the second band is slightly below 14 kDa. These two bands also appear in the peak samples. When looking at the peak sample P1, P2 and P3 it can be stated that BSA is present in all samples. The most intense band is located in the lane P2 which fits the BSA peak of the zonal chromatogram. On the other hand, the bands of the HCPs are faint. In the P1 lane a second band can be seen below BSA band and at the level of the strong HCP band of the HCP stock solution. Because this band only appears in the first peak it can be surmised that it is a positively charged protein. In the lanes for the second and third peak a HCP band at 14 kDa can be identified. This could be one the negatively charged proteins which cause the two peaks in Figure 4.12.

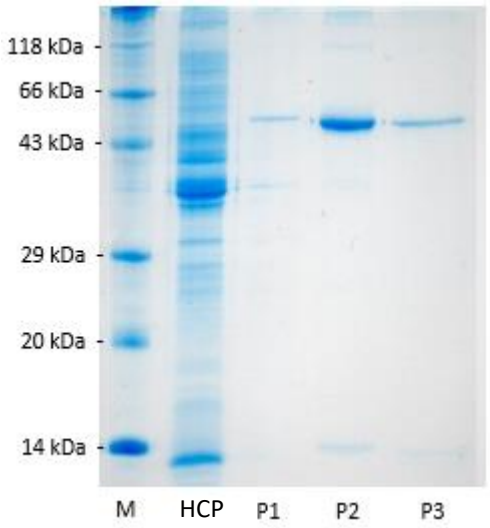

Figure 4.14: SDS-PAGE of the BSA/HCP zonal peaks

Note. M = Maker. P = Peak.

For the further evaluation the peak areas of the zonal peaks were calculated. The results are presented in Table 4.12. In contrast to the results from the experiments with BSA and LYS there are great variations in the sum of the peak area. In case of BSA and LYS a shift of the peak area size from P1 to P2 to P3 depending on the buffer could be observed tough the total peak area remains roughly the same. This shift can´t be observed with HCPs. This may be due to the inhomogeneous distribution of HCPs in the centrifuge tubes although the stock solution has been mixed well before freezing.

Table 4.12: HCP/BSA peak areas from zonal chromatography of each buffer (20 mM)

Buffer	Peak area [AV]		
	P1	P2	P3
Bis-Tris	147.50	338.60	172.80
Acetate	144.90	355.34	174.30
Carbonate	135.00	359.90	200.18
Phosphate	99.11	345.40	215.33
Imidazole	97.89	335.20	188.60
MES	96.76	336.30	140.10

Note. P = Peak

Frontal chromatography

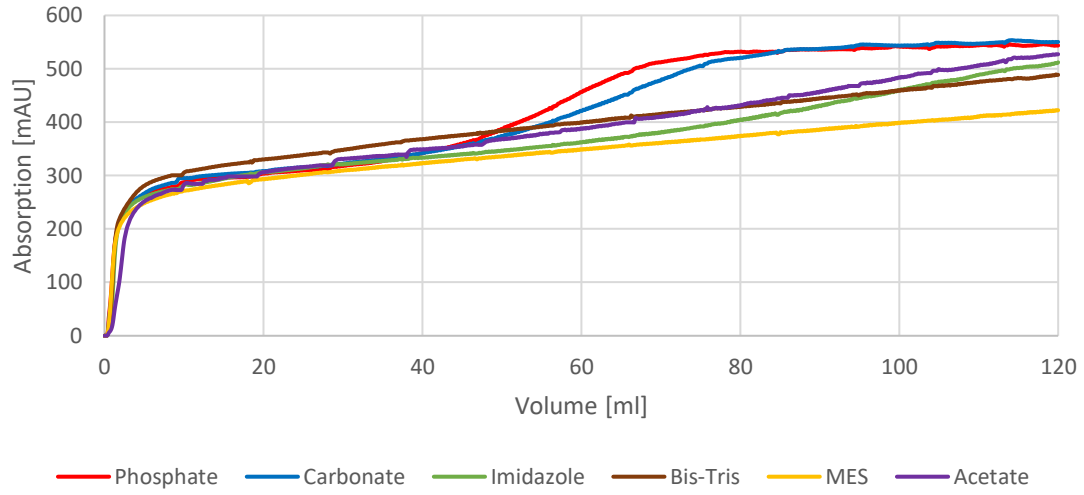

Figure 4.15: Frontal chromatography of BSA (1 mg/ml) and HCP (0.15 mg/ml) at a pH of 6.5. Flow rate = 1 ml/min. Buffer concentration = 20 mM. Column = DEAE.

Figure 4.15 shows the frontal chromatography of the protein mixture of BSA (1 mg/ml) and host cell proteins (0.15 mg/ml). As in the case of BSA/LYS, an immediate breakthrough of the proteins which are not able to bind to the column can be observed. Following to the first breakthrough, the actual BSA breakthrough curve is obtained. In contrast to the BSA/LYS experiments, no plateau is developed before the BSA breakthrough, but a steady increase of the protein concentration can be recorded. For a better evaluation of the results, the curves are set to a new baseline and are normalized to their maximum absorption. The adjustment is presented in Figure 4.16.

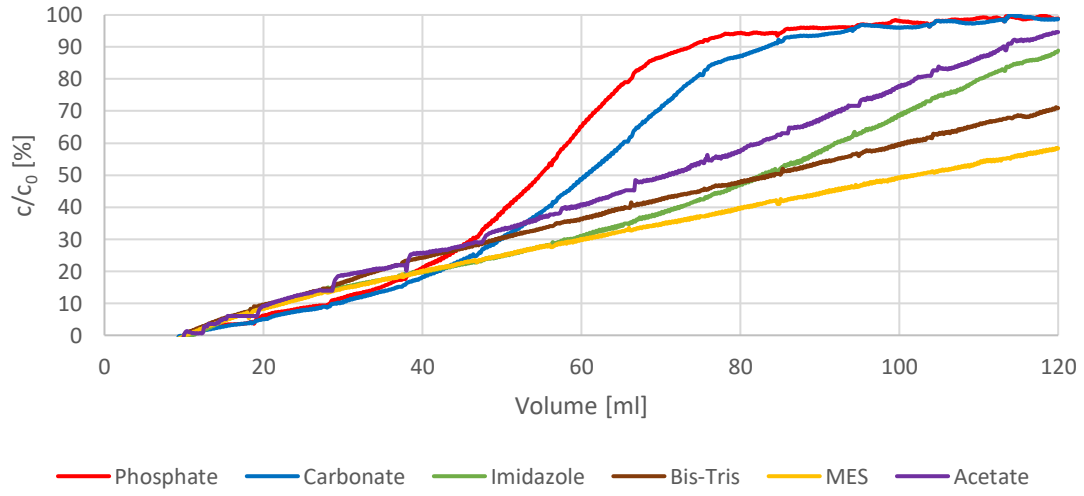

Figure 4.16: Normalized frontal chromatography and corrected baseline of BSA (1 mg/ml) and HCP (0.15 mg/ml).

Through the absence of a plateau, it was not possible to set the new baseline as precise as with LYS and BSA. Therefore, the absorption at a defined volume (10 ml) was subtracted for each curve. The phosphate and carbonate buffer still lead to the sigmoidal curve shape. With imidazole, this shape is slightly indicated. Whereas, acetate, Bis-Tris and MES have an almost linear course. By looking at the values for the $DBC_{10\%}$ it stands out that the breakthroughs appear significantly earlier compared to solely BSA and the BSA/LYS protein mixture (see Table 4.13). For the calculation of the DBC a protein concentration of 1 mg/ml is assumed. The highest $DBC_{10\%}$ of BSA/HCP (29.30 mg/ml) is achieved with carbonate, which corresponds with the $DBC_{10\%}$ of imidazole/BSA solution (29.20 mg/ml). Compared to the results from the experiments with BSA/LYS, the dynamic binding capacity of BSA in the presents of HCPs has halved. Because the HCP solution is composed of positively and negatively charged proteins, one reason for the decreased DBC could be that BSA and HCPs carrying a negative charge compete for binding sites on the column or repel each other, or the positively charged HCPs interact with BSA and the negative HCPs, thereby hindering the adsorption of BSA. Another aspect which can to be considered is that the HCPs increase the viscosity of the protein solution and thereby also influence the results (see Chapter 3.7.4). A higher viscosity of protein solution causes a decrease in protein diffusion [Wright, Muzzio & Glasser, 1998] and thus the BSA and HCP molecules can be slowed down on their way to the adsorption sites resulting in a lower dynamic binding capacity. In general, the order of the buffers remained the same compared to the “pure” BSA solution. Only the place of Bis-Tris changed from third to last. However, the differences of the $DBC_{10\%}$ between acetate, Bis-Tris, imidazole and MES are too small (≈ 1-2 mg/ml) to make a clear statement about the impact of the individual buffer salts.

Table 4.13: Comparison of the $DBC_{10\%}$ of BSA, BSA/LYS and BSA/HCP

Buffer	$DBC_{10\%}$ of BSA [mg/ml]	$DBC_{10\%}$ of BSA/LYS [mg/ml]	$DBC_{10\%}$ of BSA/HCP [mg/ml]
Carbonate	45.50	42.20	29.30
Phosphate	44.93	49.54	28.40
Bis-Tris	34.93	58.03	20.67
Imidazol	29.20	69.70	22.80
MES	25.33	51.96	21.84
Acetate	23.47	58.15	21.04

4.2.2 Troubleshooting

When first mixing lysozyme and HCPS under experimental conditions an immediate precipitation of the proteins could be observed. For the investigation of this problem different methods were utilized. Including an ion exchange and a size exclusion chromatography.

Ion Exchanger

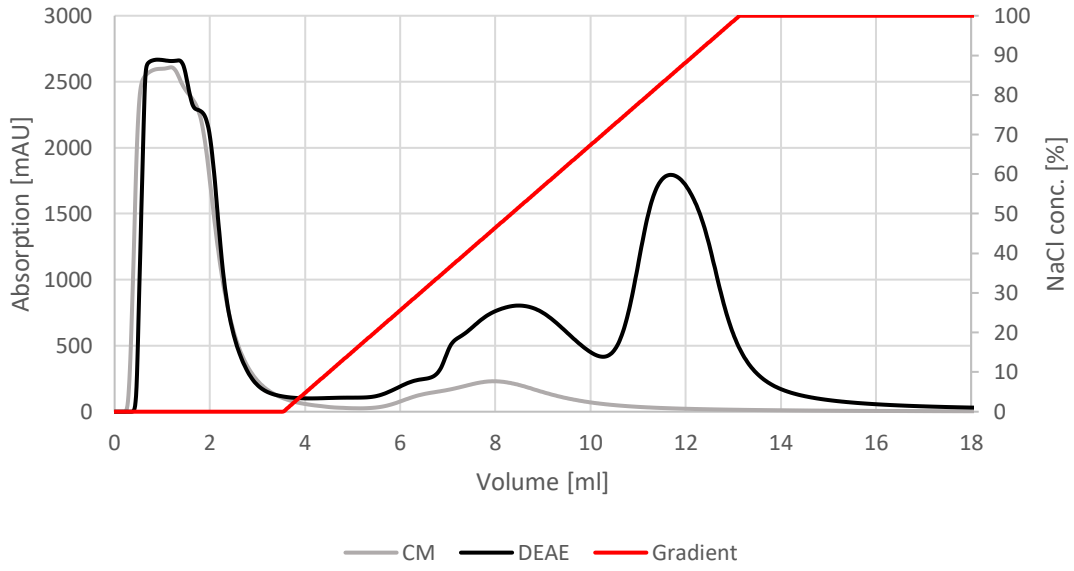

Figure 4.17: Ion exchange chromatography of HCPs using an anion (DEAE) and a cation (CM) exchanger. Sample volume = 1 ml. Flow rate = 1 ml/min. Buffer A = 20 mM Phosphate. Buffer B = 1 M NaCl.

A sample volume of 1 ml with a concentration of 7.04 mg/ml of HCPs (in 20 mM phosphate buffer) was applied on an anion (DEAE) and cation (CM) exchanger. In a first step all unbound proteins were washed out with 3 CV of 100% phosphate buffer. Hereupon the linear gradient with a length of 10 CV was run ending in a 5 VC gradient delay. Figure 4.17 shows that a great amount of proteins neither bind to the anion nor to the cation exchange column leading to an adsorption above the detection level of the ÄKTA unit (> 2600 mAU). In the further course two peaks can be observed when using the DEAE column and a single peak with the CM column. All peaks were fractionated and afterwards mixed with lysozyme. By doing this, a precipitation of proteins could be observed in the fraction containing the washed-out proteins. No precipitation took place in the fractions which were taken from the peaks during the linear gradient. This may be due to the higher salt

concentration caused by buffer B. For a further investigation of the impact of the salt concentration on the precipitation, additional buffer trails were performed.

Buffer salt trials

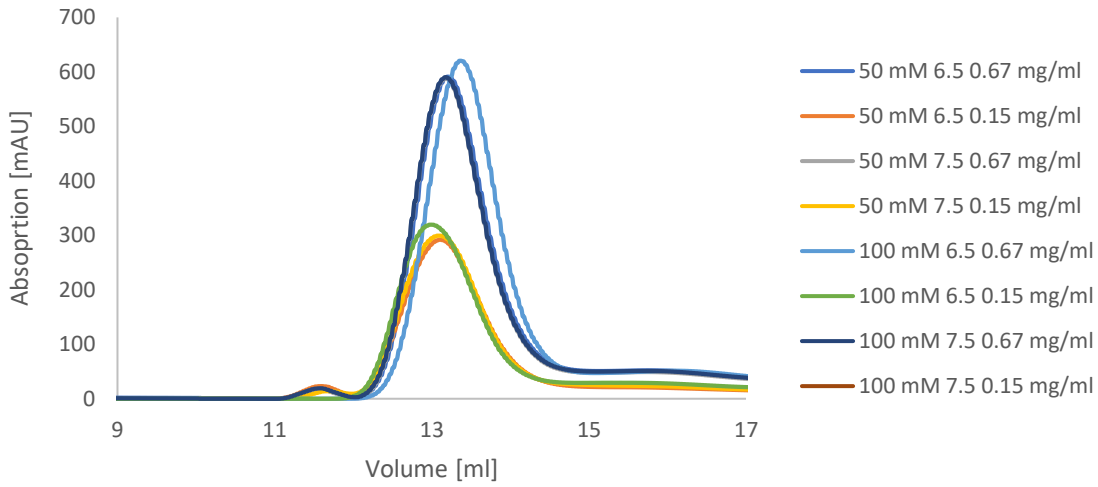

Figure 4.18: SEC chromatogram of the buffer change containing HCP. Flow rate = 3 ml/min. Sample volume = 1 ml. Fraction volume = 1.5 ml. Buffer concentrations: 50 and 100 mM phosphate. pH = 6.5 and 7.5. Protein concentration = 0.70 and 0.15 mg/ml.

For the buffer salt verification, the ÄKTA start and a SEC column (HiTrap™ desalting 5 ml) were utilized. Figure 4.18 displays the protein peaks which were fractionated during the buffer change from PBS to 50/100 mM phosphate buffer. Each peak is collected half as fraction 5 and 6. Additionally two different HCP concentration were examined. As concentrations a 1:10 dilution (0.70 mg/ml) und the working concentration (0.15 mg/ml) were chosen. Table 4.15 shows the results of the 1:10 dilution. In fraction no. 5 a precipitation took place at every salt concentration and pH after the addition of lysozyme. In fraction no. 6 no precipitation could be observed at the highest salt concentrations. These differences are likely to be caused by different HCP concentrations in fraction no. 5 and 6.

Table 4.14: 0.70 mg/ml phosphate buffer

Fraction of SEC	20 mM pH 6.5	50 mM pH 6.5	100 mM pH 6.5	50 mM pH 7.5	100 mM pH 7.5
5	+	+	+	+	+
6	+	+	-	+	-

Note. + : precipitation. - : no precipitation.

In Table 4.16 the results of the 0.15 mg/ml concentration are presented. In the 5th fraction no precipitation took place only at 100 mM phosphate and pH 7.5. In fraction no. 6 there was no precipitation with the highest buffer salt concentration (100 mM) and at pH 7.5.

Table 4.15: 0.15 mg/ml (+ precipitation, - no precipitation) phosphate buffer

Fraction of SEC	20 mM pH 6.5	50 mM pH 6.5	100 mM pH 6.5	50 mM pH 7.5	100 mM pH 7.5
5	+	+	+	+	-
6	+	+	-	-	-

Note. + : precipitation. - : no precipitation.

The results which were observed during these buffer salt trails may be described by the salting-in effect. This phenomenon describes the increasing solubility of a protein with the salt concentration in the solution. Salting-in takes place at low ion concentrations when salt is added. The added salt shields the proteins charge and thereby weakens the interactions between the proteins themselves. This shielding effect can prevent aggregation and precipitation. The pH also has an influence on the salting-in. The effect is stronger when the pH is closer to the pI of the protein. When increasing the salt concentration salting-out occurs, leading to the opposite effect [Kramer et al., 2012]. This would explain why the best results are achieved at pH 7.5 and 100 mM phosphate salt concentration. It can be assumed that the salt ions shield lysozyme and the HCPs from each other and thus restrain their interaction and preventing the precipitation of the proteins. A similar effect could be observed during the molarity trails. With a higher salt concentration, the protein solution containing lysozyme became clearer. In the solution with solely BSA no turbidity or salting-in effect was observed. An explanation for the behavior if lysozyme can be its high positive net charge compared to BSA.

These results also correspond with published protocols for cell distribution which can be found in literature. For example, *Feliu, Cubarsi & Villaverde* (1998) use a disruption buffer containing 50 mM Tris-HCL, 10 mM $MgCl_2$, 100 mM NaCl and 10 mM β-mercaptoethanol at pH 7.2. The higher salt concentration need to avoid precipitation however, is not consistent with the previous experimental conditions. Therefore, the use of the cation exchanger in combinations with HCPs and lysozyme must be waived.

4.3 Molarity trials

In this series of experiments, different buffer molarities at a constant pH has been investigated. To this end the buffers carbonate, MES and imidazole were chosen. Carbonate often showed the best dynamic binding capacities whereas, MES and imidazole have varying results. Moreover, these buffers were selected because they all have different charge attributes. Carbonate is negatively charged, imidazole positively and MES is a zwitterion. The changes of the molarity were both applied on the anion and cation exchanger. The buffers were adjusted to the following molarities: 10 mM, 20 mM, 30 mM and 50 mM. Those values are often found in literature e.g. Herrmann (2002), Rösch et al. (2016) and Meissner et al. (2015). Whereby, 20 mM is used as the reference value. Since a protein mixture of BSA and lysozyme is applied, all breakthrough curves are set to a new baseline. The protein concentration remained the same as before.

The same set of experiments were performed also with BSA and HCP. However, during the experiments the DEAE Sepharose FF column broke, leading to instant breakthrough of the protein solution. Therefore, the results were rejected. Due to lack of time these experiments were not repeated.

4.3.1 Carbonate

Anion exchanger

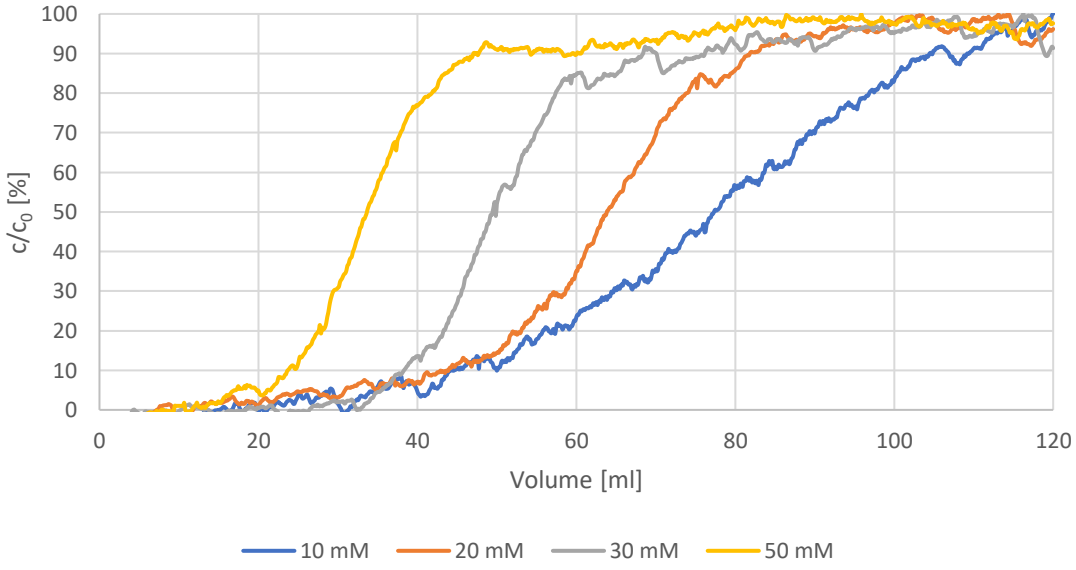

Figure 4.19: Frontal chromatography of different molarities of carbonate with BSA (1 mg/ml) and LYS (1 mg/ml). BTC minus the adsorption of LYS. Flow rate = 1 ml/min. Buffer concentration= 10 mM, 20 mM, 30 mM and 50 mM. pH = 6.5. Column = DEAE.

In this figure the breakthrough curves of the different molarities of carbonate are plotted. Except for the 10 mM concentration, all BTC show the sigmoidal curve progression. Breakthrough of BSA/LYS starts earlier with increasing the carbonate concentration. The values for the $DBC_{10\%}$ and the percentage change in comparison to the 20 mM concentration are shown in Table 4.16. The best $DBC_{10\%}$ with 44.24 mg/ml has the carbonate concentration of 10 mM followed by 20 mM and 30 mM (- 9.05%). The $DBC_{10\%}$ is almost halved. In this case, it can be said that with increasing ionic strength the dynamic binding capacity degreases. This agrees with evidence found in literature [Shi et al., 2005] and [Harinarayan et al., 2006]. The lower DBC at higher salt concentration can be caused by the effect that the anions enhance the repulsion between the BSA molecules in solution. Additionally, the repulsion can take place between BSA molecule which are adsorbed by the stationary phase and molecules which are still in solution. Through the shielding of lysozyme by the anions the effect is supported. At low salt concentrations lysozyme can act as a "buffer" between the BSA molecules, strengthening the interactions of BSA with the column matrix and a development of protein layer can take place.

Table 4.16: Characteristics and $DBC_{10\%}$ of BSA/LYS at different molarities of carbonate from the DEAE column

Concentration [mM]	Charge [mM]	Conductivity [mS/cm]	$DBC_{10\%}$ [mg/ml]	Percentage [%]
10	- 5.86	2.12	44.24	+ 4.83
20	- 11.71	3.35	42.20	0
30	- 17.57	5.46	38.38	- 9.05
50	- 29.28	8.82	23.73	- 43.77

Cation exchanger

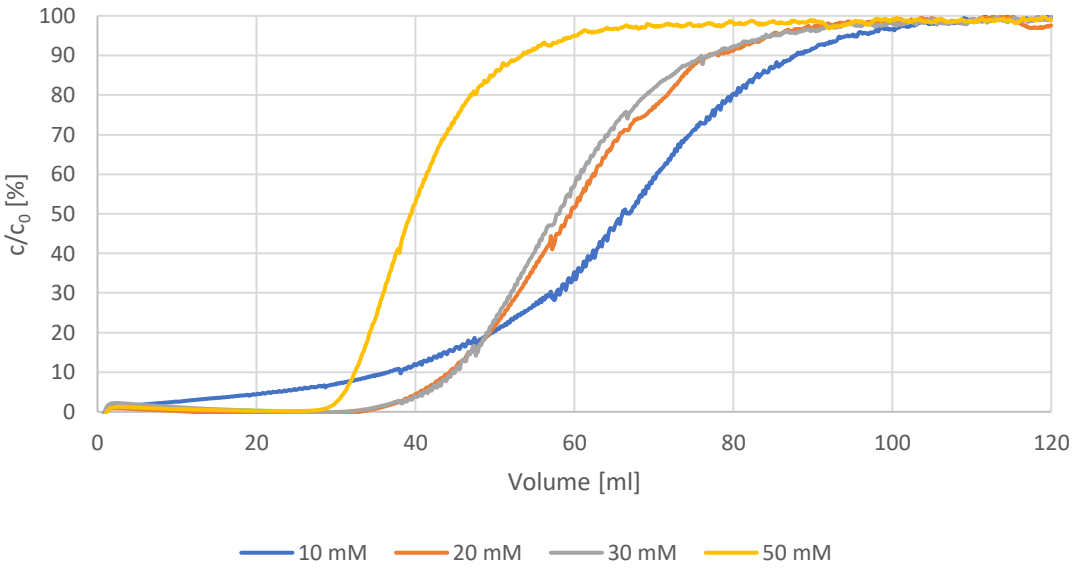

Figure 4.20: Frontal chromatography of different molarities of carbonate with LYS (2 mg/ml) and BSA (1 mg/ml). BTC minus the adsorption of BSA. Flow rate = 1 ml/min. Buffer concentration = 10 mM, 20 mM, 30 mM and 50 mM. pH = 6.5. Column = CM.

In the case of the cation exchanger all four received breakthrough curves are sigmoidal (see Figure 4.20). However, the 10 mM curve shows almost an immediate increase of the protein concentration at the outlet of the column from the beginning of the application. Though, the point of 10% breakthrough isn´t reached until 36 ml. The course of the BTC of 20 mM and 30 mM are almost identical as well as their $DBC_{10\%}$ (see Table 4.17). Again, the 50 mM buffer salt concentration leads to the earliest but also steepest breakthrough. Regarding these results the assumption could be made that there is a competition between the shielding effect of the anions and an increase of the column´s zeta potential by lysozyme. Through the adsorption of positively charged lysozyme, the negative charge of the column gets overlaid. In case of the 10 mM concentration, the share of ions is too low to compensate the change of the zeta potential caused by the positively charged lysozyme. At 50 mM the anions are mostly acting on the lysozyme and thereby lowering its zeta potential. Both effects lead to a decrease of the dynamic binding capacity. Additionally, the negative charge of BSA is reducing the zeta potential of lysozyme, too. But this is only an additive, since the concentration of BSA remains constant.

Table 4.17: Characteristics and $DBC_{10\%}$ of BSA/LYS at different molarities of carbonate from the CM column

Concentration [mM]	Charge [mM]	Conductivity [mS/cm]	$DBC_{10\%}$ [mg/ml]	Percentage [%]
10	- 5.86	2.12	73.34	- 17.91
20	- 11.71	3.35	89.34	0
30	- 17.57	5.46	90.04	+ 0.78
50	- 29.28	8.82	64.80	- 27.47

4.3.2 MES

Anion exchanger

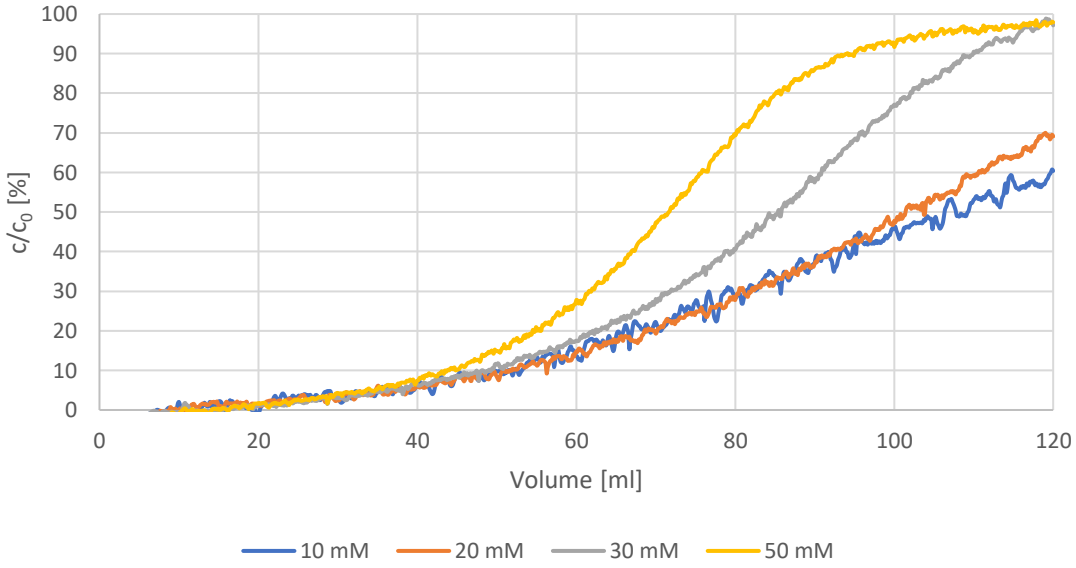

Figure 4.21: Frontal chromatography of different molarities of MES with BSA (1 mg/ml) and LYS (1 mg/ml). BTC minus the adsorption of LYS. Flow rate = 1 ml/min. Buffer concentration = 10 mM, 20 mM, 30 mM and 50 mM. pH = 6.5. Column = DEAE.

Figure 4.21 shows the results from molarity trials of MES on the DEAE FF column. A significant change of the breakthrough curve from the buffer salt concentration from 10 mM to 50 mM can be observed. With increasing buffer molarity, the curve to a more sigmoidal form. However, the moment of 10% breakthrough only slightly shifts to an earlier position (see Table 4.18). The difference between the worst and best $DBC_{10\%}$ is only about 8 mg/ml, although the share of anions is greater compared to carbonate. Maybe the zwitterionic property of MES (positively charged amino group and a negatively charged sulfonyl group) weakens the effect of the increased ionic strength. At low MES concentration the share of monovalent ions, compared to zwitterionic ion, is greater than

at high concentrations. One additional possibility could be that the MES ions arrange themselves like a “lipid membrane” around the BSA molecules (amino group facing BSA/sulfonyl group facing outwards), maintaining its negative charge. At the same time the monovalent anions can act as a shield for the positively charged lysozyme leading to repulsion of BSA and LYS and thereby, hindering the adsorption. At low salt concentrations (10 and 20 mM) this effect is weaker.

Table 4.18: Characteristics and $DBC_{10\%}$ of BSA/LYS at different molarities of MES from the DEAE column

Concentration [mM]	Charge [mM]	Conductivity [mS/cm]	$DBC_{10\%}$ [mg/ml]	Percentage [%]
10	- 7.15	0.85	51.74	- 0.42
20	- 14.31	1.02	51.96	0
30	- 21.46	1.75	48.13	- 7.37
50	- 35.76	2.41	43.85	- 15.61

Cation exchanger

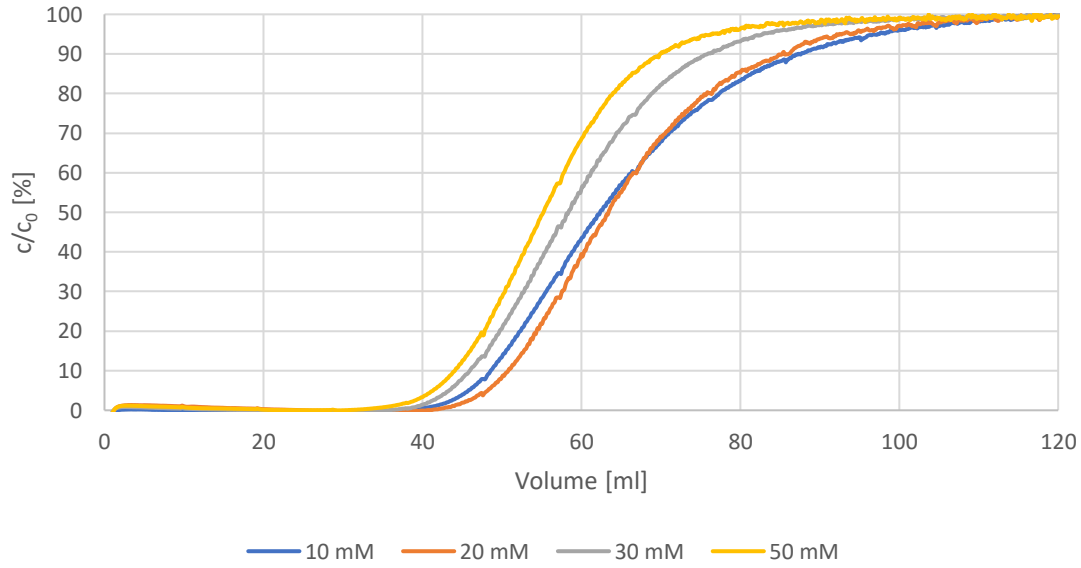

Figure 4.22: Frontal chromatography of different molarities of MES with LYS (2 mg/ml) and BSA (1 mg/ml). BTC minus the adsorption of BSA. Flow rate = 1 ml/min. Buffer concentration = 10 mM, 20 mM, 30 mM and 50 mM. pH = 6.5. Column = CM.

The results from the cation exchanger CM FF are quite different compared to the anion exchanger. All four received breakthrough curves have the typical S-shape and the volume at which the 10% breakthrough is reached, is in a range of 7 ml (see Figure 4.22). In combination with Table 4.19 it can be seen that the decrease and increase of the molarity both lead to a decline of the $DBC_{10\%}$. The 10 mM buffer salt concentration has the second

best result with 97.26 mg/ml which means only a deterioration of 4.31 % compared to the 20 mM. The trend is comparable to the results of carbonate/cation exchanger, even though the influence of MES seems to have a smaller impact. The same assumption which was made for the anion exchanger could be true for this case. With the difference that the zwitterions arrange themselves the other way around (sulfonyl group facing lysozyme/ amino group facing outwards).

Table 4.19: Characteristics and $DBC_{10\%}$ of BSA/LYS at different molarities of MES from the CM column

Concentration [mM]	Charge [mM]	Conductivity [mS/cm]	$DBC_{10\%}$ [mg/ml]	Percentage [%]
10	- 7.15	0.85	97.26	- 4.31
20	- 14.31	1.02	101.44	0
30	- 21.46	1.75	91.92	- 9.56
50	- 35.76	2.41	88.54	- 12.89

4.3.3 Imidazol

Anion exchanger

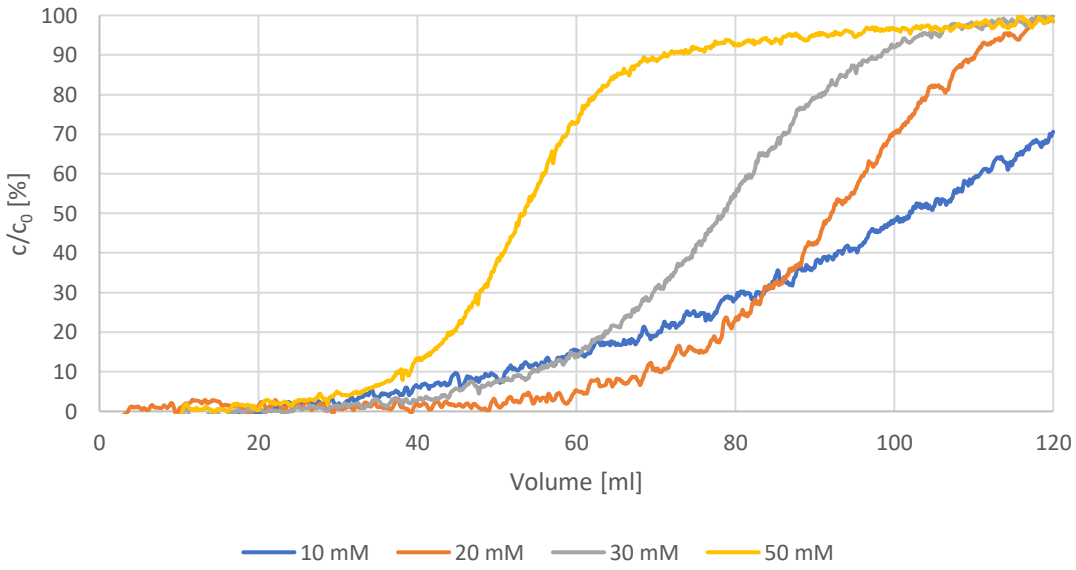

Figure 4.23: Frontal chromatography of different molarities of imidazole with BSA (1 mg/ml) and LYS (1 mg/ml). BTC minus the adsorption of LYS. Flow rate = 1 ml/min. Buffer concentration = 10 mM, 20 mM, 30 mM and 50 mM. pH 6.5. Column = DEAE.

The last buffer to be investigated is imidazole. As with the other buffers, a change of the curve shape with increasing salt concentration can be observed. At the same time, an earlier breakthrough is caused by that (see Figure 4.23). With imidazole those differences

are greater than with carbonate and MES. Table 4.20 shows that an alternation of 10 mM of the buffer salt concentration leads to deterioration of 25.43 % (10 mM) and 20.81 % (30 mM) of the dynamic binding capacity at 10 % breakthrough. At a molarity of 50 mM imidazole, the best curve shape is achieved but the $DBC_{10\%}$ is almost halved compared to 20 mM. Because imidazole is oppositely charged to BSA, the same behavior as carbonate/MES with the cation exchanger should be observed. With increasing imidazole concentration, the cations act as a shield around BSA weakening its electrostatic interaction with the stationary phase and/or enhancing the repulsions to lysozyme leading the less adsorbed BSA molecules because of missing built up of protein layer.

Table 4.20: Characteristics and $DBC_{10\%}$ of BSA/LYS at different molarities of imidazole from the DEAE column

Concentration [mM]	Charge [mM]	Conductivity [mS/cm]	$DBC_{10\%}$ [mg/ml]	Percentage [%]
10	+ 7.38	0.91	51.22	- 25.43
20	+ 14.76	1.34	68.70	0
30	+ 22.14	1.82	54.48	- 20.81
50	+ 36. 91	2.98	37.72	- 45.09

Cation exchanger

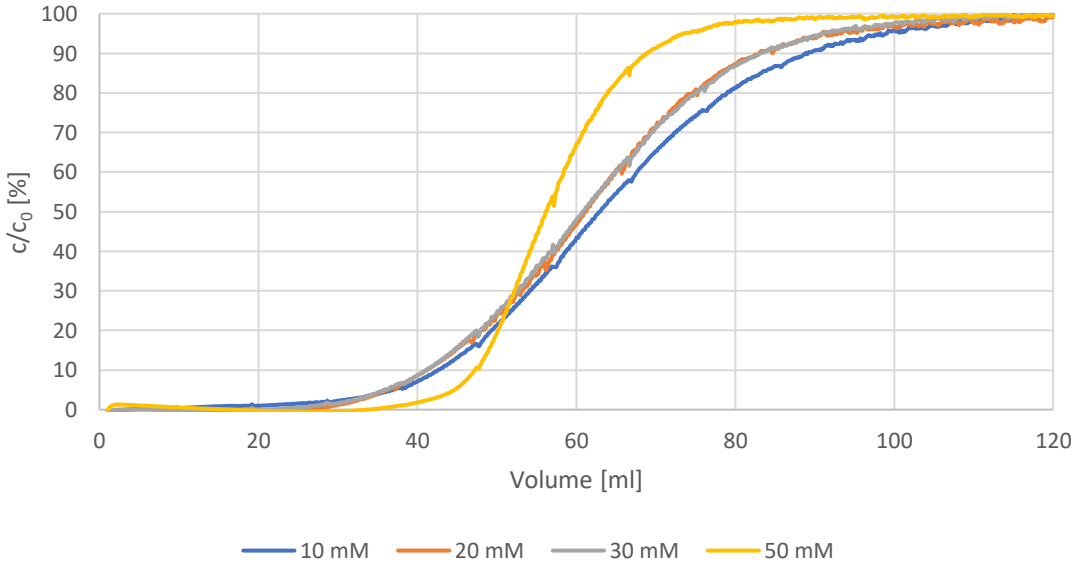

Figure 4.24: Frontal chromatography of different molarities of imidazole with LYS (2 mg/ml) and BSA (1 mg/ml). BTC minus the adsorption of BSA. Flow rate = 1 ml/min. Buffer concentration: 10 mM, 20 mM, 30 mM and 50 mM. pH = 6.5. Column = CM.

Figure 4.24 shows the results of different imidazole concentration in combination with the cation exchanger. In comparison to all previous molarity trails, the differences between the individual buffer salt concentration are the smallest. Furthermore, only increases of the $DBC_{10\%}$ could be recorded (see Table 4.21). The most obvious improvement was obtained with 50 mM imidazole. With this concentration the steepest breakthrough curve and concurrent highest dynamic binding capacity was received. This is reflected in the dynamic binding capacity which amounts 94.26 mg/ml. Compared to 20 mM (82.36 mg/ml), this is an increase of 14.89%. The increased concentration of imidazole could have the positive effect that it shields the negative charge of BSA and thereby, inhibiting the interaction of BSA and lysozyme, resulting in a higher number of lysozyme molecules which are able to be adsorbed without limitation by the stationary phase. Thus, a steeper course of the breakthrough curve can be observed.

Table 4.21: Characteristics and $DBC_{10\%}$ of BSA/LYS at different molarities of imidazole from the CM column

Concentration [mM]	Charge [mM]	Conductivity [mS/cm]	$DBC_{10\%}$ [mg/ml]	Percentage [%]
10	+ 7.38	0.91	85.30	+ 3.57
20	+ 14.76	1.34	82.36	0
30	+ 22.14	1.82	82.44	+ 0.10
50	+ 36. 91	2.98	94.26	+ 14.89

4.4 pH trials

In this test series the buffer salt concentration remained constant at 20 mM, but the pH value was change from 6.5 to 7.5. Again, the effect on the buffers carbonate, MES and imidazole was investigated. Both an anion and cation exchanger were utilized. Since a protein mixture of BSA and lysozyme is applied, all breakthrough curves were set to a new baseline.

4.4.1 Carbonate

Anion exchanger

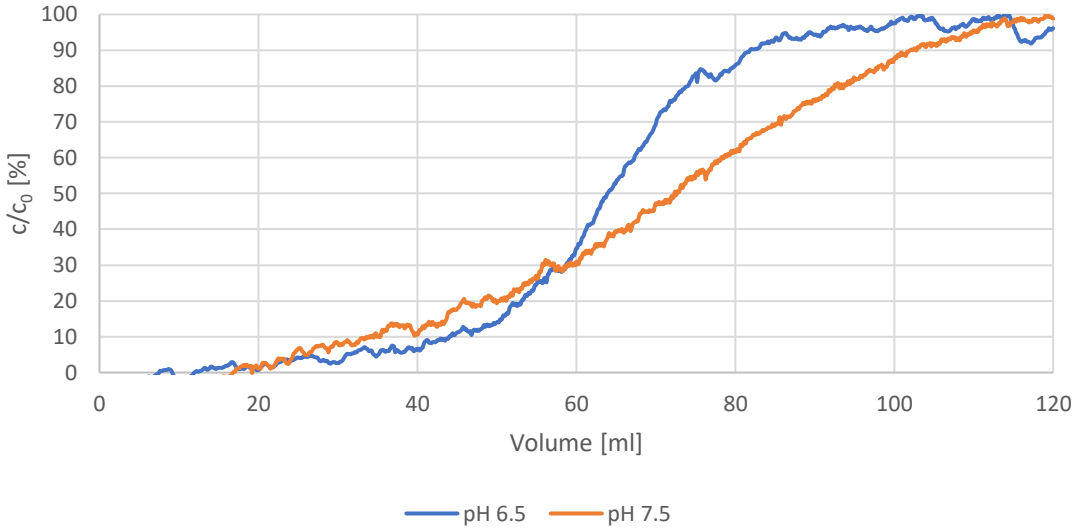

Figure 4.25: Frontal chromatography of different pH of carbonate with BSA (1 mg/ml) and LYS (1 mg/ml). BTC minus the adsorption of LYS. Flow rate = 1 ml/min. Buffer concentration: 20 mM. pH = 6.5, 7.5. Column: DEAE.

Figure 4.25 shows that due to the change of the pH-value from 6.5 to 7.5, the breakthrough curve loses its sigmoidal shape and doesn´t end in a plateau in the giving time. This results in an earlier breakthrough and thus a lower dynamic binding capacity. Compared to pH 6.5, the $DBC_{10\%}$ of pH 7.5 is 19.43 % lower (see Table 4.22). By increasing the pH to 7.5 the net charge of BSA decreases from -13 to -17 [Shi et al., 2005] and thereby the electrostatic interaction between the adsorber and BSA should increase, leading to an improved DBC. The presents of lysozyme seem to undermine this proposed mechanism because of its positive charge. The change of the overall net charge of lysozyme is small in comparison to BSA [Yu, Liu & Zhou, 2015] *Rösch et al.* (2017) state that at a higher pH the formation of agglomerates between BSA and lysozyme is more pronounced (in the presents of anions) leading to more molecule complexes with an increase of size. Thus, earlier pore blockage occurs and the number of BSA/LYS molecules which can be absorbed deeper into the pores is slowed down.

Table 4.22: Characteristics and $DBC_{10\%}$ of BSA/LYS at different pH of 20 mM carbonate from the DEAE column

pH	Charge [mM]	Conductivity [mS/cm]	$DBC_{10\%}$ [mg/ml]	Percentage [%]
6.5	- 11.71	3.35	42.20	0
7.5	- 18.68	4.16	34.00	- 19.43

Cation exchanger

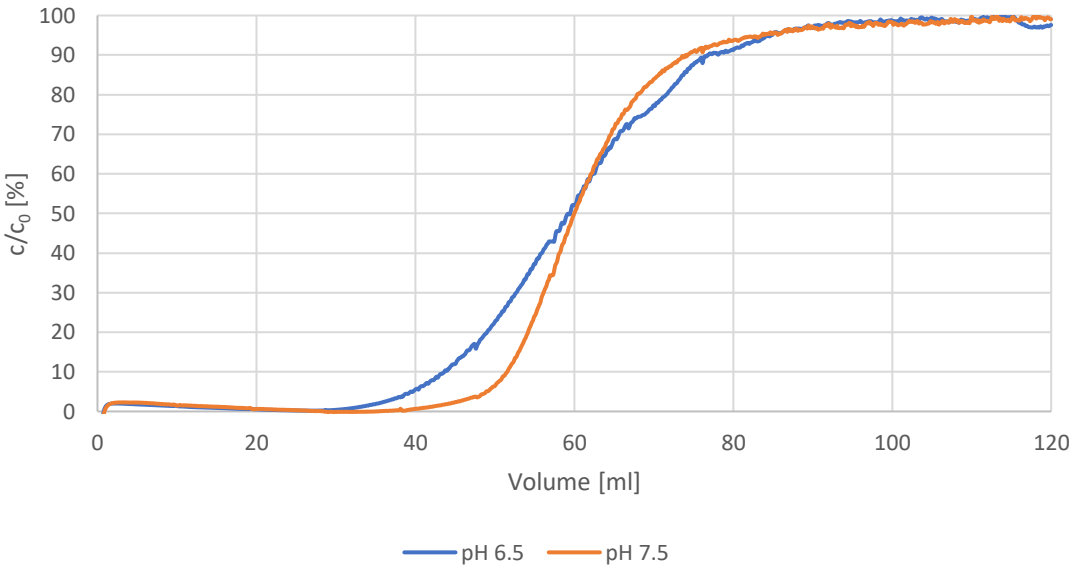

Figure 4.26: Frontal chromatography of different pH of carbonate with LYS (2 mg/ml) and BSA (1 mg/ml). BTC minus the adsorption of BSA. Flow rate = 1 ml/min. Buffer concentration = 20 mM. pH = 6.5, 7.5. Column = CM.

In contrast to the anion exchanger, a positive effect caused by the pH change can be observed (see Figure 4.26). The breakthrough of the pH 7.5-curve occurs later, and the subsequent course of the curve is steeper. Because of the difference in size and molecular mass of BSA and lysozyme, lysozyme can be absorbed faster, so that the formation of agglomerates can occurs directly at the column. This might enable the development of a protein layer of lysozyme/BSA and thereby an increase of the dynamic binding capacity. Table 4.23 shows that an improvement of 15.47% was achieved even though the share of monovalent anions is greater at this pH. However, the interactions of the proteins seem to have a more distinct influence.

Table 4.23: Characteristics and $DBC_{10\%}$ of BSA/LYS at different pH of 20 mM carbonate from the CM column

pH	Charge [mM]	Conductivity [mS/cm]	$DBC_{10\%}$ [mg/ml]	Percentage [%]
6.5	- 11.71	3.35	89.34	0
7.5	- 18.68	4.16	103.16	+ 15.47

4.4.2 MES

Anion exchanger

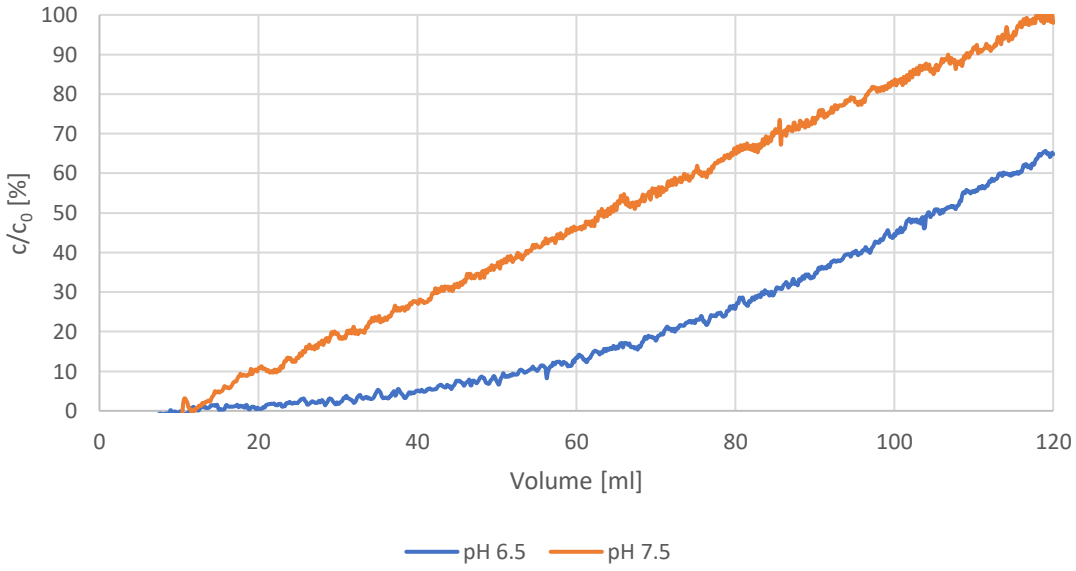

Figure 4.27: Frontal chromatography of different pH of MES with BSA (1 mg/ml) and LYS (1 mg/ml). BTC minus the adsorption of LYS. Flow rate = 1 ml/min. Buffer concentration = 20 mM. pH = 6.5, 7.5. Column = DEAE.

As can be seen in Figure 4.27, the adjustment of the buffer to the pH of 7.5 leads to a significant deterioration of the breakthrough curve of BSA which is almost completely straight. As a result, the dynamic binding capacity decreases from 51.96 mg/ml to 19.67 mg/ml (see Table 4.24). At this pH, the buffer solution consists almost completely of monovalent ions leading to the similar trend which could already be observed with the carbonate buffer. Though, the deterioration of the dynamic binding capacity is much greater (-62.75%) which could be caused by slightly higher share of monovalent anions. And again, the zwitterionic property of MES can have an influence here.

Table 4.24: Characteristics and $DBC_{10\%}$ of BSA/LYS at different pH of 20 mM MES from the DEAE column

pH	Charge [mM]	Conductivity [mS/cm]	$DBC_{10\%}$ [mg/ml]	Percentage [%]
6.5	- 14.31	1.02	52.80	0
7.5	- 19.23	1.53	19.67	- 62.75

Cation exchanger

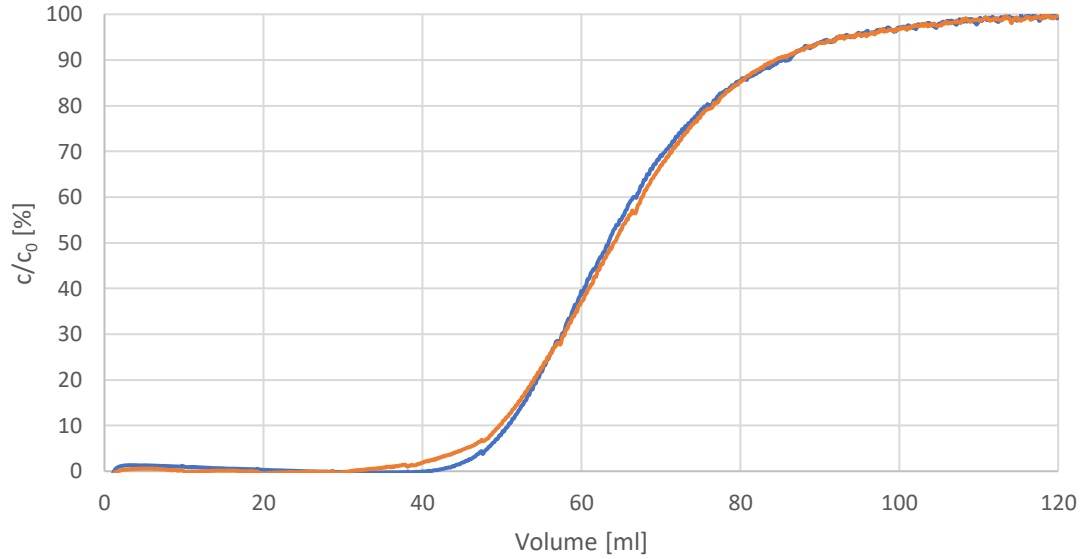

Figure 4.28: Frontal chromatography of different pH of MES with LYS (2 mg/ml) and BSA (1 mg/ml). BTC minus the adsorption of BSA. Flow rate = 1 ml/min. Buffer concentration = 20 mM. pH = 6.5, 7.5. Column = CM.

The raise of the pH-value to 7.5 leads to almost no change of the breakthrough curve regarding the form and the dynamic binding capacity. The DBC decreases only by 1.42 % (see Figure 4.28 and Table 4.25). The increased share of MES anions seems to cancel out the benefit of the greater number of protein complexes.

Table 4.25: Characteristics and $DBC_{10\%}$ of BSA/LYS at different pH of 20 mM MES from the CM column

pH	Charge [mM]	Conductivity [mS/cm]	$DBC_{10\%}$ [mg/ml]	Percentage [%]
6.5	- 14.31	1.02	101.44	0
7.5	- 19.23	1.53	100	- 1.42

4.4.3 Imidazole

Anion exchanger

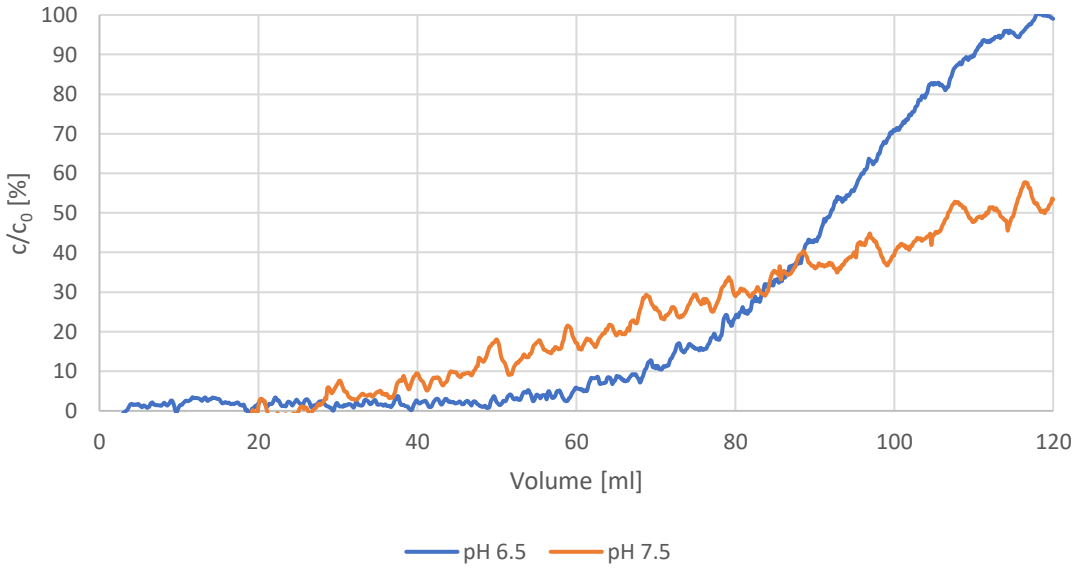

Figure 4.29: Frontal chromatography of different pH of imidazole with BSA (1 mg/ml) and LYS (1 mg/ml). BTC minus the adsorption of LYS. Flow rate = 1 ml/min. Buffer concentration = 20 mM. pH = 6.5, 7.5. Column = DEAE.

As with the previous pH trails on the anion exchanger, the pH change causes a deterioration of the breakthrough curve (see Figure 4.29). In this case, the BTC of "pH 7.5" reaches only 55 % of c/c_0 after a volume of 120 ml has been applied on the column and the curve lost completely its sigmoidal curve shape. Table 2.26 shows the pH change results in a decrease of the $DBC_{10\%}$ of 31.34 % and the share of cations is reduced to 4.40 mM (see Table 4.16). As with carbonate and MES the increases share of protein complexes consisting of BSA and LYS leads to a significant decrease of the dynamic binding capacity.

Table 4.26: Characteristics and $DBC_{10\%}$ of BSA/LYS at different pH of 20 mM imidazole from the DEAE column

pH	Charge [mM]	Conductivity [mS/cm]	$DBC_{10\%}$ [mg/ml]	Percentage [%]
6.5	+ 14.76	1.34	68.70	0
7.5	+ 4.40	0.24	47.17	- 31.34

Cation exchanger

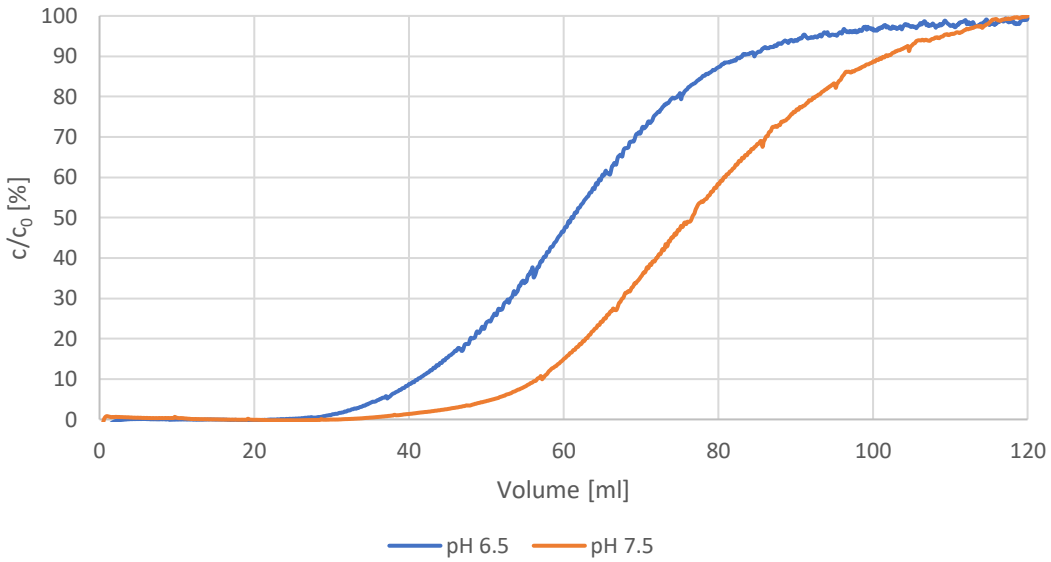

Figure 4.30: Frontal chromatography of different pH of imidazole with LYS (2 mg/ml) and BSA (1 mg/ml). BTC minus the adsorption of BSA. Flow rate = 1 ml/min. Buffer concentration = 20 mM. pH = 6.5, 7.5. Column = CM.

In case of the cation exchanger a positive development of the breakthrough curve can be observed by changing the pH from 6.5 to 7.5 of the imidazole buffer solution (see Figure 4.30). The volume at which 10 % breakthrough is attained has increases significantly. In Table 4.27 it is shown that the $DBC_{10\%}$ has improved by 26.30 %. With 113.28 mg/ml the best dynamic binding capacity of all frontal chromatographic runs has been achieved. The lower concentration of ions could have the positive effect that lysozyme and BSA can build up a protein layer without be disturbed by shielding or competitive binding of ions. It also has to be kept in mind that the lysozyme concentration is twice as high as the BSA concentration when using the cation exchanger. This could also favor the increase of the dynamic binding capacity.

Table 4.27: Characteristics and $DBC_{10\%}$ of BSA/LYS at different pH of 20 mM imidazole from the CM column

pH	Charge [mM]	Conductivity [mS/cm]	$DBC_{10\%}$ [mg/ml]	Percentage [%]
6.5	+ 14.76	1.34	89.69	0
7.5	+ 4.40	0.24	113.28	+ 26.30

5. Conclusion

Throughout the experiments several factors have been identified to have an impact on the dynamic and static binding capacity. Starting with the size and the charge of the protein itself. Small proteins like lysozyme (14.3 kDa) can be adsorbed better by the stationary phase than larger proteins like BSA (66.2 kDa). With small proteins the blockage of pores happens at a later time, allowing a greater number of protein molecules to penetrate the pores. This statement is verified by the "blank" runs of BSA and lysozyme. The DBC and SBC of lysozyme are in average 2.6 times and 1.8 times higher than the values of BSA. When applying a solution containing BSA and lysozyme, the interaction of both proteins with each other lead to a change of the DBC and SBC as well. The form of interaction can be expressed in the formation of protein-complexes or protein layers. For BSA an increase of 63 % in average can be noted and for lysozyme a decrease of 19 %. The impact of on the SBC is scientifically smaller (± 2 %). The above-mentioned formation of protein complexes and layers seem to influence the DBC rather than the SBC (see Table 5.1).

Table 5.1: Average values for the $DBC_{10\%}$ and SBC of each protein solution

Protein (column)	BSA (DEAE)	BSA/LYS (DEAE)	BSA/HCP (DEAE)	LYS (CM)	LYS/BSA (CM)
$DBC_{10\%}$ [mg/ml]	33.89	55.39	24.01	88.73	71.66
SBC [mg/ml]	66.04	65.14	-	120.25	123.40

Another influencing variable are the buffer salts. Depending on charge and ionic strength of the buffers, different results concerning the DBC and SBC can be observed. Though the dynamic and static binding capacity never follow the same order. This can be ascribed to the fact that different adsorption kinetics take place at the beginning of sample application compared to the later phase. Regarding the dynamic binding capacity, it can be observed that the influence of the shielding effect of ions charged oppositely to the protein is stronger than the competitive binding of ions to the opposite charged stationary phase. The better results for BSA and lysozyme were achieved with buffer having a medium ionic strength and ions carrying the same charge as the protein, with exception of MES whose zwitterionic property seems to have negative impact on the DBC. However, the presence

of an additional protein (BSA or LYS) causes that the buffer ions carrying the same charge as the additional protein lead to the better result of the DBC. This draws the conclusion that for the isolation of a single protein from a protein mixture, it is of advantage to use a buffer which carries the same charge as the desired protein.

A further factor which is of interest, is the impact of different buffer salt molarities and the pH of the buffer solution. In the most cases both, a too low or too high concentration of buffer salts lead to a decrease of the dynamic binding capacity. At moderate buffer salt concentration (50 mM) the shielding effect of the ions regarding the protein gets stronger. Also, the influence on the zeta potential grows. If the zeta potential of an object shifts towards zero, the electrostatic interactions with another charged object decreases. Since ion exchange chromatography is based on the interaction of charged materials, it is from importance to sustain a sufficient zeta potential of opposite charge for the stationary phase and the protein. For that reason, an unnecessary high concentration of buffer salt should be avoided. During the molarity trials a significant deterioration of the DBC was observed at the buffer salt concentration of 50 mM. The only exception being imidazole in combination with the cation exchanger which yielded the best DBC at 50 mM buffer concentration.

When choosing the pH, the pI of the protein should be considered. Due to the pH change from 6.5 to 7.5 the overall net charge of BSA became more negative, leading to an increased formation of protein complexes consisting of BSA and LYS. In case of the anion exchanger this caused a significant decrease of the dynamic binding capacity. For the cation exchanger an increase of the DBC could be observed which can be explained by the greater share of adsorbed BSA molecules. Therefore, the isolation of a single protein is more effective at a pH which is closer to the pI of the stronger charged protein.

A comparison of the different breakthrough curves under the above described conditions are presented in Figure 5.1 – 5.6.

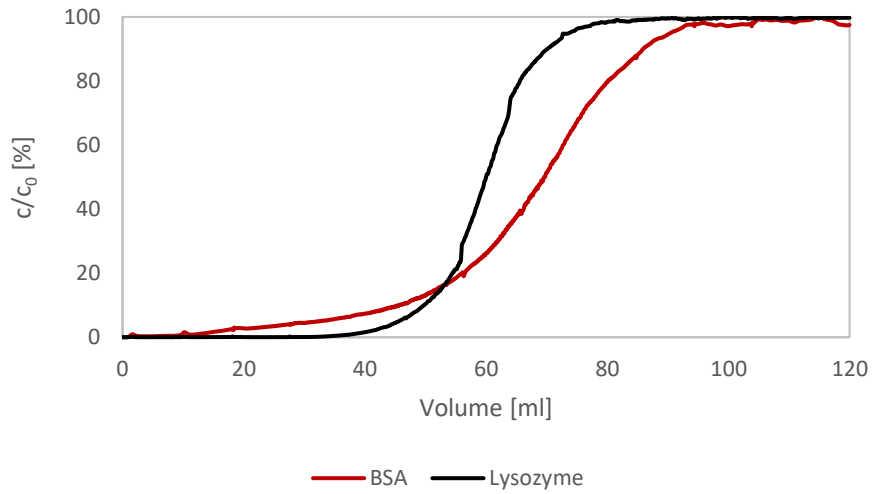

Figure 5.1: Breakthrough curve of BSA (1 mg/ml) and LYS (2 mg/ml). Flow rate = 1 ml/min. Buffer: 20 mM carbonate. pH = 6.5. Column: DEAE (BSA) and CM (LYS).

Figure 5.1 shows the breakthrough curves of the small protein lysozyme and the bigger protein BSA in 20 mM carbonate buffer and at pH 6.5. The first part of the curve for lysozyme is closer to the x-axis and the form of the curve is much more symmetric compared to the BSA curve. This indicates a better adsorption of lysozyme than of BSA. This can be explained by the faster adsorption of small molecules compared to large molecules.

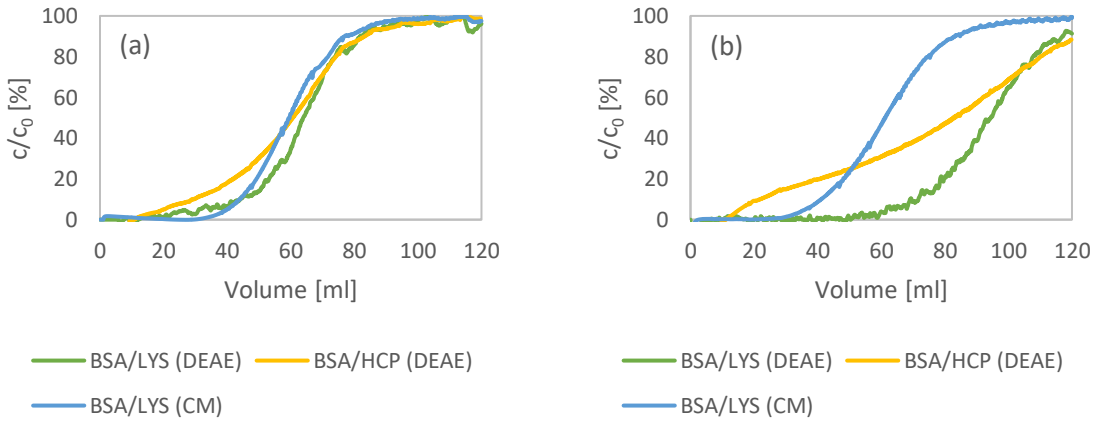

Figure 5.2: Comparison of the breakthrough curved under the influence of monovalent anions and monovalent cations on different protein solutions and columns. (a) 20 mM carbonate. (b) 20 mM imidazole. Flow rate = 1 ml/min. pH = 6.5.

In this Figure the impact of monovalent anions (a) and cations (b) on the breakthrough curves of different protein solutions is compared. Through the change from anions to cations the BTC of BSA/LYS on the anion exchanger shifts significantly to the right. Whereas, on the cation exchanger the same protein solution undergoes a shift in the opposite

direction (decrease of the DBC). On the DEAE column the use of carbonate leads to shielding of positive lysozyme. Therefore, the formation of an BSA/LYS complex is hampered, and less protein is adsorbed by the stationary phase. When changing to imidazole this shielding effect of lysozyme is missing and enables the interaction of lysozyme and BSA. This again leads to higher number proteins which can bind to the column. In the case of the cation exchanger the same observation can be made but to a smaller extent. But with carbonate the DBC is higher than with imidazole. This also concludes that lysozyme has a positive influence on the DBC of BSA but BSA a negative impact on LYS. For BSA/HCP this consideration is more difficult to apply because the HCP solution contains negatively and positively charged proteins. However, imidazole seems to have a strong influence on the binding capacity of the HCPs.

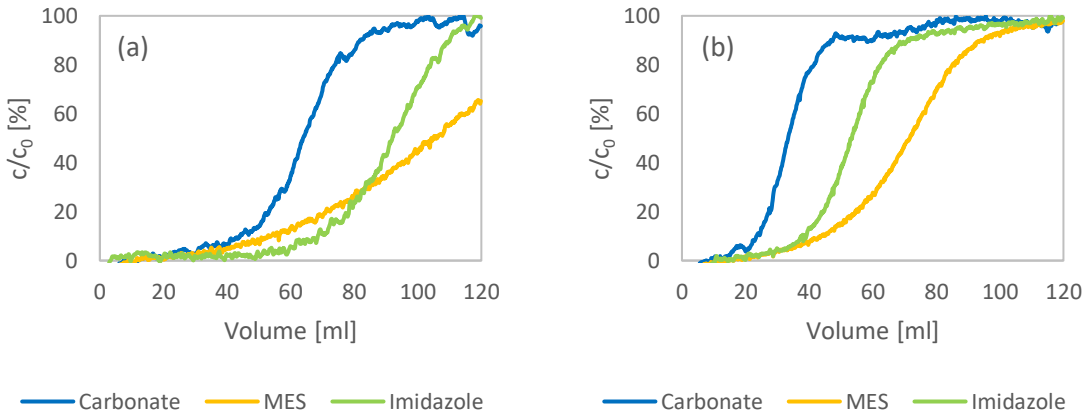

Figure 5.3: Comparison of the breakthrough curves of different carbonate, MES and imidazole concentrations on the anion exchanger. (a) Buffer concentration = 20 mM. (b) Buffer concentration = 50 mM. Flow rate = 1 ml/min. pH = 6.5. BSA = 1 mg/ml. LYS = 1 mg/ml.

In Figure 5.3 the influence of the buffer salt concentration on the dynamic binding capacity is presented. The change from 20 mM (a) to 50 mM (d) of all three puffers caused a decrease of DBC. For carbonate and MES the explanation can be found in enhanced shielding of lysozyme. For imidazole the increase of the salt concentration may have led to a shielding of the BSA molecule which is stronger than the force to interact with lysozyme.

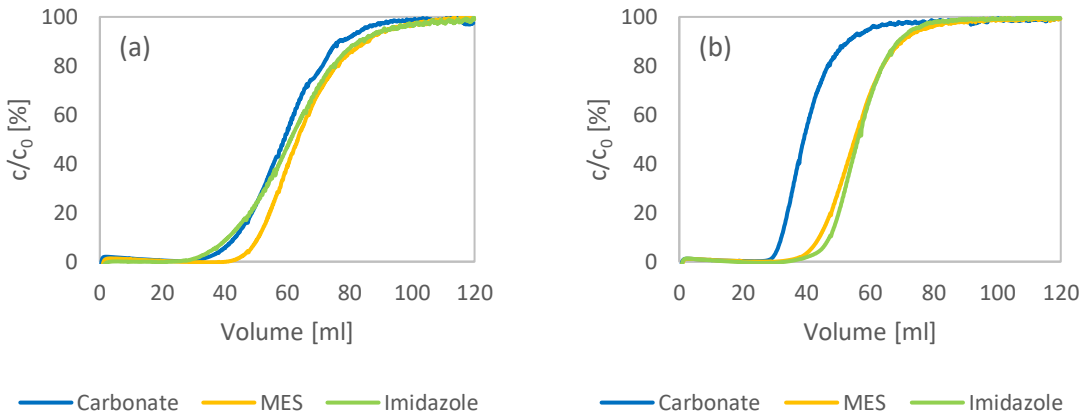

Figure 5.4: Comparison of the breakthrough curves of different carbonate, MES and imidazole concentrations on the cation exchanger. (a) Buffer concentration = 20 mM. (b) Buffer concentration = 50 mM. Flow rate = 1 ml/min. pH = 6.5. BSA = 1 mg/ml. LYS = 2 mg/ml.

In Figure 5.4 the impact of buffer concentration in the presence of the cation exchanger is investigated. The increase of the buffer concentration to 50 mM lead to a decrease of the DBC for carbonate and MES by shielding the lysozyme molecules. However, for imidazole an improved DBC can be observed. The higher share of cation on the other hand could cause a better shielding of BSA which enables an increased adsorption of lysozyme. The $DBC_{10\%}$ value of BSA/LYS and 50 mM imidazole corresponds with the value of solely lysozyme and imidazole.

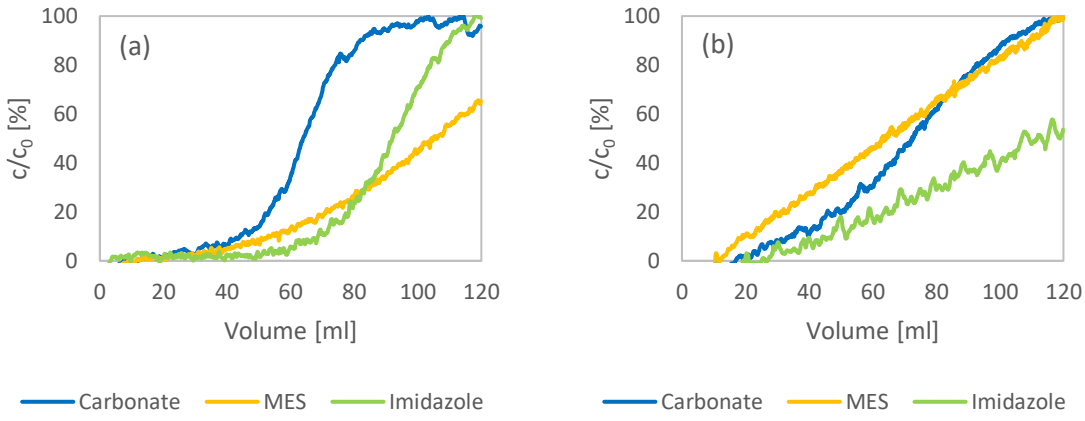

Figure 5.5: Comparison of the breakthrough curves of different pH of carbonate, MES and imidazole on the anion exchanger. (a) pH = 6.5. (b) pH = 7.5. Flow rate = 1 ml/min. Buffer concentration = 20 mM. BSA = 1 mg/ml. LYS = 1 mg/ml.

In case of a pH change from 6.5 (a) to 7.5 (b) a significant deterioration of the dynamic binding capacity of BSA/LYS/DEAE can be observed (see Figure 5.5). As mention in Chapter 4.4.1 the formation of agglomerates of BSA and lysozyme increases with higher pH. The

greater number of protein complexes lead to an earlier blockage of the adsorber pores and the dynamic binding capacity decreases significantly.

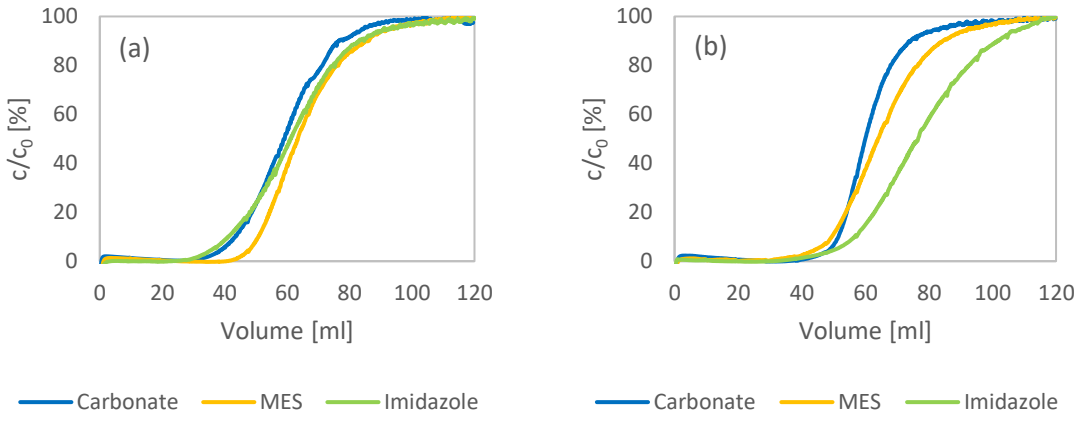

Figure 5.6: Comparison of the breakthrough curves of different pH of carbonate, MES and imidazole on the cation exchanger. (a) pH = 6.5. (b) pH = 7.5. Flow rate = 1 ml/min. Buffer concentration = 20 mM. BSA = 1 mg/ml. LYS = 2 mg/ml.

For the cation exchanger the opposite trend of the anion exchanger can be observed (see Figure 5.6). The dynamic binding capacity increases. The assumption is that the interaction of lysozyme and BSA takes place after a part of the lysozyme molecules is already adsorped onto the column due to its smaller size. In the further process the BSA molecules interaction with the adsorbed lysozyme, enabling the adsorption of more lysozyme molecules onto BSA.

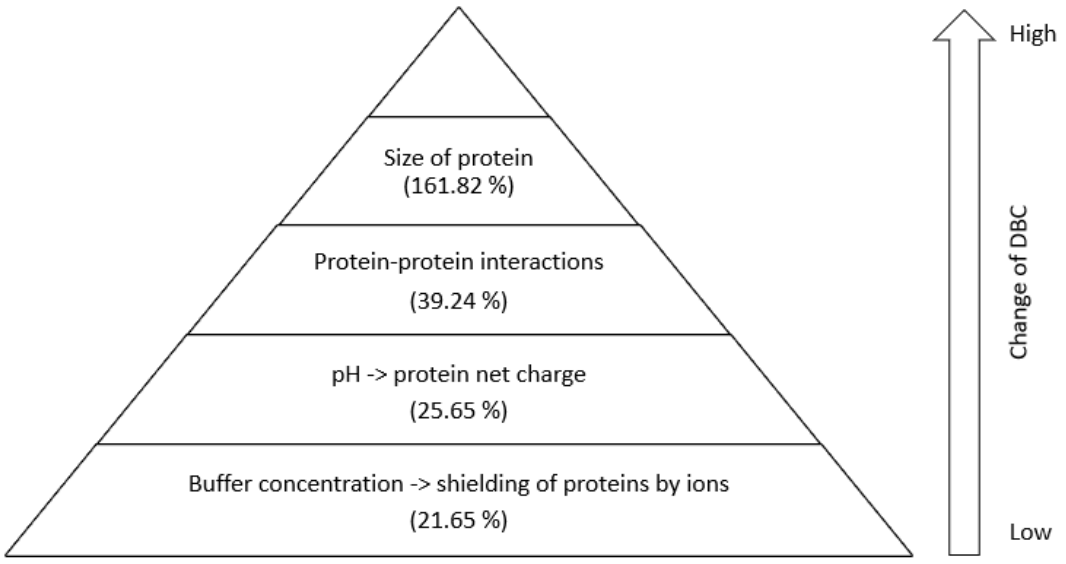

Figure 5.7: Order of influencing values sorted by the percentage change of the DBC from bottom to top.

Taking the above mention impacts and the average percentage change of the DBC into account, the following order can be established (see Figure 5.7). The average DBC value of 20 mM buffer salt concentration and pH 6.5 serve as a basis for the calculation of the DBC change. The lowest impact is located at the bottom of the pyramid. With an average change of the DBC of ± 21.65% the shielding of the proteins by anions and cations depending on the buffer concentration shows the least influence during these experiments. Followed by change of the pH and thus the change of the proteins net charge with ± 25.65%. A further influencing factor which was identified are the protein-protein interactions. They caused an average change of the DBC by ± 39.24%. At the head of the pyramid is the impact of the size of the Protein. The dynamic binding capacity of lysozyme is in average 161.82% higher than the one of BSA.

For further experiments it could be of interest to evaluate the protein-protein interaction in dependence of the salt type and concentration by employing a SEC. Therefore, the elution peak of the frontal chromatography from the IEXC could be applied on a size exclusion column. In turn the SEC elution peaks could provide information on the cooperative adsorption of the proteins.

References

ÄKTApurifier. (2018, March 15). Retrieved from Ge Healthcare Life Sciences: http://legacy.gelifesciences.com/webapp/wcs/stores/servlet/catalog/en/GELifeSciences-de/products/AlternativeProductStructure_17162/28406271

Anspach, B. (2012). *Deutsches Skript zur Vorlesung Protein Purification / Preparative Chromatography.* Unpublished script, Hochschule für Angewandte Wissenschaften: Fakultät Life Sciences, Hamburg.

Biological buffers. (2018, January 30). Retrieved from Reach Devices: http://www.reachdevices.com/Protein/BiologicalBuffers.html

Biological buffers. (2018, Febuary 18). Retrieved from Applichem: https://www.google.de/url?sa=t&rct=j&q=&esrc=s&source=web&cd=1&ved=0ahUKEwj-8I6YoLDZAhVGKuwKHem-DugQFggnMAA&url=https%3A%2F%2Fwww.applichem.com%2Ffileadmin%2FBroschueren%2FBioBuffer.pdf&usg=AOvVaw1rqV633IHMrz6Q0lxXTkR9

Burns, D., & Zydney, A. (1999). Buffer effects on the zeta potential of ultrafiltration membranes. *Journal of Membrane Science*, 39-48.

Carta, G., & Jungbauer, A. (2010). *Protein Chromatography: Process Development and Scale-Up.* Weinheim: Wiley-VCH.

Cazes, J. (2001). *Encyclopedia of Chromatography.* New York: Marcel Dekker Inc.

Dismer, F., & Hubbuch, J. (2007). A novel approach to characterize the binding orientation of lysozyme on ion-exchange resins. *Journal of Chromatography A*, 312-320.

Dismer, F., Petzold, M., & Hubbuch, J. (2008). Effects of ionic strength and mobile phase pH on the binding orientation of lysozyme on different ion-exchange adsorbents. *Journal of Chromatography A*, 11-21.

E 262 - sodium acetate. (2018, January 31). Retrieved from Enius: http://www.enius.de/lexikon/e262.html

Faude, A., Zacher, D., Müller, E., & Böttinger, H. (2007). Fast determination of conditions for maximum dynamic capacity in cation-exchange chromatography of human monoclonal antibodies. *Journal of Chromatography*, 29-35.

Feliu, J., Cubarsi, R., & Villaverde, A. (1998). Optimized Release of Recombinant Proteins by Ultrasonication of E. coli Cells. *Biotechnology and Bioengineering*, 536-540.

Freitag, R. (2014). Chromatographic Techniques in the Downstream Processing of Proteins in Biotechnology. In R. Pötner, *Animal Cell Biotechnology: Methods and Protocols, Methods in Molecular Biology.* Luxemburg: Springer Science+Business Media, LLC.

Gossett, P., Rizvi, S., & Baker, R. (1984). Quantitative Analysis of Gelation in Egg Protein Systems. *Food Technology* , 67-96.

Grushka, E., & Grinber, N. (2014). *Advances in Chromatography.* Boca Raton: CRC Press.

Hanke, A., & Ottens, M. (2014). Purifying biopharmaceuticals: knowledge-based chromatographic process development. *Trends in Biotechnology*, 210-220.

Harinarayan, C., Mueller, J., Ljunglöf, A., Fahrner, R., van Alstine, J., & van Reis, R. (2006). An Exclusion Mechanism in IOn Exchange Chromatography. *Biotechnology and Bioengineering*, 775-787.

Herrmann, T. (2002). Diplomarbeit. Braunschweig: TU Braunschweig.

HiTrap CM Sepharose FF. (2018, January 31). Retrieved from GE Healthcare Life Science: https://cdn.gelifesciences.com/dmm3bwsv3/AssetStream.aspx?mediaformatid=10061&destinationid=10016&assetid=12944

HiTrap DEAE Sepharose FF. (2018, February 8). Retrieved from GE Healthcare Life Science: https://cdn.gelifesciences.com/dmm3bwsv3/AssetStream.aspx?mediaformatid=10061&destinationid=10016&assetid=12944

Huang, B., Kim, H., & Dass, C. (2004). Probing three-dimensional structure of bovine serum albumin by chemical cross-linking and mass spectrometry. *Journal of the American Society for Mass Spectrometry*, 1237-1247.

Inamuddin, & Luqman, M. (2014). *Ion Exchange Technology II: Applications.* Berlin: Springer.

Instruction for use: Roti-Quant. (2018, April 12). Retrieved from Carl Roth: https://www.carlroth.com/downloads/ba/de/K/BA_K015_DE.pdf

Interpreting protein binding capacities for chromatography media (resins). (2018, January 31). Retrieved from GE Healthcare Life Science: http://proteins.gelifesciences.com/protein-blog-and-news/protein-skills-blog/interpreting-protein-binding-capacities/

Kramer, R., Shende, V., Motl, N., Pace, N., & Scholtz, M. (2012). oward a Molecular Understanding of Protein Solubility: Increased Negative Surface Charge Correlates with Increased Solubility. *Biophysical Journal*, 1907-1915.

Lundanes, E., Reubsaet, L., & Greibrokk, T. (2013). *Chromatography: Basic Principles, Sample Preperations and Related Methods.* Weinheim: Wiley-VCH.

Lysozyme. (2018, January 30). Retrieved from Sigma Aldrich: http://www.sigmaaldrich.com/catalog/product/sigma/l3790?lang=de&region=DE

Majorek, K., Porebski, P., Dayal, A., Zimmerman, M., Jablonska, K., Stewart, A., . . . Minor, W. (2012). Structural and immunologic characterization of bovine, horse, and rabbit serum albumin. *Molecular immunilogy*, 174-182.

Mashhori Ghaleh Babakhani, N. (2017). *Der Einfluss von Puffersalzen in der Frontalchromatographie an einem Anionaustauscher*. Hochschule für Angewante Wissenschaften, Hamburg.

Meissner, J., Prause, A., Bharti, B., & Findenegg, G. (2015). Characterization of protein adsorption onto silica nanoparticles: influence of pH and ionic strength. *Colloid and Polymer Science*, 2281-3391.

Mohan, C. (2006). *Buffers. A guide for the preparation and use of buffers in biological systems.* San Diego: EMD Bioscience.

Mortimer, C., & Mueller, U. (2010). *Chemie.* Stuttgart: Thieme.

Niu, H. (n.d.). Effect of buffer on protein capture with weak cation exchanger membranes. Ontario, Canada: University of Waterloo.

Palacio, L., Ho, C., Prádanos, P., Hernández, A., & Zydney, A. (2003). Fouling with protein mixtures in microfiltration: BSA–lysozyme and BSA–pepsin. *Journal of Membrane Science*, 41-51.

Patra, S., Santhosh, K., Pabbathi, A., & Samanta, A. (2012). Diffusion of organic dyes in bovine serum albumin solution studied by fluorescence correlation spectroscopy. *RSC Advances*, 6079-6086.

Phillips, D. (1967). The Hen Egg-White Lysozyme Molecule. *National Academy of Sciences*, 483-495.

Ratnaparkhi, M., Chaudhari, S., & Panday, V. (2011). Peptides and Proteins in Pharmaceuticlas. *International Journal of Current Pharmaceutical Research*, 1-9.

Robards, K., Haddad, P., & Jackson, P. (2004). *Principles and Practice of Modern Chromatography Methods.* London: Elsevier Ltd.

Rösch, C., Kratz, F., Hering, T., Trautmann, S., Umanskaya, N., Tippkötter, N., . . . Ziegler, C. (2016). Albumin-lysozyme interactions: Cooperative adsorption on titaniumand enzymatic activity. *Colloids and Surfaces B: Biointerfaces*, 115-121.

Salgin, S., Salgin, U., & Bahadir, S. (2012). Zeta Potentials and Isoelectric Points of Biomolecules: The Effects of Ion Types and Ionic Strengths. *International Journal of Electrochemical Science*, 12404-12414.

Sekhon, B. S. (2010). Biopharmaceuticals: an overview. *Thai Journal of Pharmaceutical Sciences*, 1-19.

Sepahi, M., Kaghazian, H., Sereshkeh, M., Sadeghcheh, T., Hadadian, S., Jebeli, M., & Yacari, F. (2014). Optimization of Dynamic Binding Capacity of Anion Exchange Chromatography Media for Recombinant Erythropoietin Purification. *Iranian Journal of Biotechnology*, 49-55.

Shi, Q., Zhou, Y., & Sun, Y. (2005). Influence of pH and ionic strength on the steric mass-action model parameters around the isoelectric point of protein. *Biotechnology progress*, 516-523.

Skidmore, G., Horstmann, B., & Chase, H. (1989). Modelling single-component protein adsorption to the cation exchanger S Sepharose FF. *Journal of Chromatography*, 113-128.

Tsumoto, K., Ejima, D., Senczuk, A., Kita, Y., & Arakawa, T. (2006). Effects of Salts on Protein–Surface Interactions: Applications for Column Chromatography. *Journal of Pharmaceutical Sciences*, 1677-1690.

Wang, X., & Hunter, A. M. (2009). Host Cell Proteins in Biologics Development: Identification, Quantitation and Risk Assessment. *Biotechnology and Bioengineering*, 446-458.

Westermeier, R., & Gronau, S. (2005). *Electrophoresis in practice: a guide to methods and applications of DNA and protein seperations.* Weinheim: Wiley-VCH.

Wright, P., Muzzio, F., & Glasser, B. (1998). Batch Uptake of Lysozyme: Effect of Solution Viscosity and Mass Transfer on Adsorption. *Biotechnology Progress*, 913-921.

Yu, G., Liu, J., & Zhou, J. (2015). Mesoscopic Coarse-Grained Simulations of Hydrophobic Charge Induction Chromatography (HCIC) for Protein Purification. *AIChE Journal* , 2035-2047.

Zor, T., & Selinger, Z. (1995). Linearization of the Bradford protein assay increases its sensitivity: theoretical and experimental studies. *Analystical Biochemistry*, 302-308.

List of figures

List of tables

Appendix

A.1 Digital Version

Eidesstattliche Versicherung

Hiermit versichere ich an Eides statt, dass ich die vorliegende Masterarbeit selbständig und ohne unerlaubte Hilfe von Dritten erstellt habe. Andere als in der Masterarbeit angegebenen Hilfsmitteln wurden nicht herangezogen. Alle Stellen, die sinngemäß oder direkt aus fremden Quellen entnommen sind, sind entsprechend gekennzeichnet.

Hamburg, den 27.04.2018 Unterschrift: